Review

Comprehensive Insights into Photoreforming of Waste Plastics for Hydrogen Production

Huiyao Wang *

Posted Date: 17 April 2025

doi: 10.20944/preprints202504.1506.v1

Keywords: Plastic Photoreforming; Waste Valorization; Semiconductor Photocatalysts; Microplastic Degradation; Circular Economy; Photocatalyst Design; Sustainable Hydrogen; Techno-Economic Analysis

 doi:10.20944/preprints202504.1506.v1

Review

Comprehensive Insights into Photoreforming of Waste Plastics for Hydrogen Production

E.M.N. Thiloka Edirisooriya, Punhasa S. Senanayake, Tarek Ahasan, Pei Xu and Huiyao Wang *

Department of Civil Engineering, New Mexico State University, 3035 S Espina St, Las Cruces, NM 88003, United States

* Correspondence: huiyao@nmsu.edu

Abstract: The global plastic crisis, characterized by over 400 million metric tons of annual production and low recycling rates, has evolved into a pressing environmental and energy challenge. Photocatalytic plastic photoreforming presents a dual-benefit strategy that transforms non-recyclable waste plastics into hydrogen fuel and valuable organic byproducts using solar energy under mild conditions. This review critically examines recent advances in photocatalyst design, including semiconductors, metal-organic frameworks-derived composites, and co-catalyst systems, alongside emerging insights into polymer degradation pathways and reactor configurations. Key operational parameters such as pH, light intensity, flow dynamics, and substrate properties are analyzed for their influence on hydrogen yields and byproduct selectivity. Life-cycle assessment and techno-economic analysis reveal that while current photoreforming systems face hurdles related to quantum efficiency, scalability, and cost competitiveness, innovations in material synthesis, light management, and integrated system design offer promising solutions. The potential to upcycle complex plastic waste into hydrogen aligns photoreforming with circular economy principles, particularly if combined with policy incentives and advanced separation strategies to mitigate environmental risks. With the convergence of environmental remediation and renewable energy production, plastic photoreforming emerges as a viable contributor to sustainable hydrogen economies.

Keywords: plastic photoreforming; waste valorization; semiconductor photocatalysts; microplastic degradation; circular economy; photocatalyst design; sustainable hydrogen; techno-economic analysis

1. Introduction

The rapid expansion of plastic production and consumption over the past century has culminated in a critical global plastic waste crisis. In 2023, global plastic production reached 413.8-428.7 million metric tons, with projections indicating a continued increase at a compound annual growth rate of 6.2% from 2023 to 2028 (Figure 1) [1]. The annual volume of mismanaged plastic waste is projected to increase by approximately 86%, exacerbating environmental pollution and ecological degradation. Concurrently, greenhouse gas (GHG) emissions from the global plastic lifecycle are expected to rise significantly, from 1.9 gigatons of carbon dioxide equivalent ($GtCO_2e$) per year in 2019 to 3.1 $GtCO_2e$ by 2040, representing a 63% increase [2]. This surge in emissions, driven by plastic production, waste mismanagement, and end-of-life treatment processes such as incineration, poses a substantial challenge to climate change mitigation efforts. One of the most critical concerns associated with plastic waste is its environmental persistence. Unlike organic materials, plastics exhibit extremely slow degradation rates, fragmenting into microplastics that pose significant ecological and health risks. These microplastics have the potential for bioaccumulation and biomagnification, infiltrating food chains and posing a threat to both aquatic and terrestrial organisms [3]. Addressing the global plastic waste crisis requires an integrated approach that includes improved waste management strategies, innovative recycling and reusing technologies, policy interventions, and public awareness campaigns.

 doi:10.20944/preprints202504.1506.v1

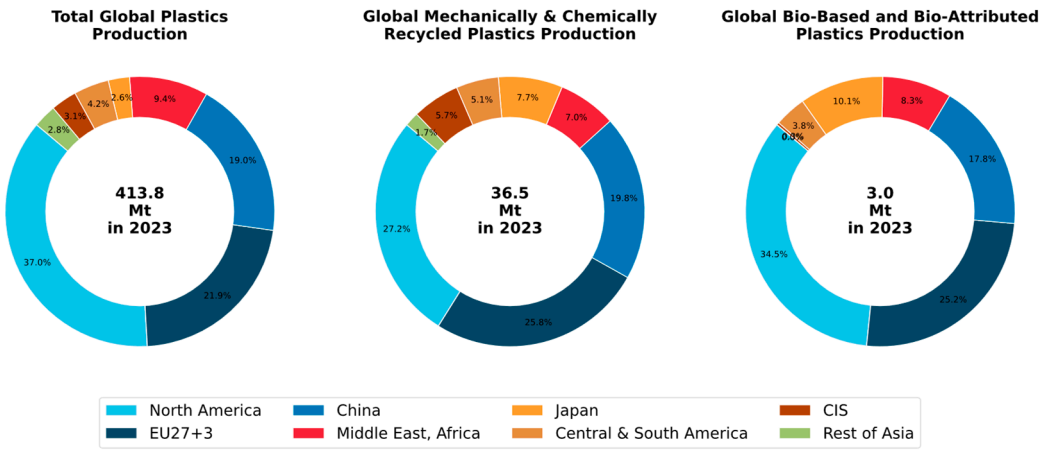

Figure 1. Global share of total plastic and bio-based plastic production, with recycled production [4].

Reusing waste plastic as a feedstock material for hydrogen (H_2) production, combined with carbon capture and storage, is one technology option to address the plastic waste challenge. H2 is a vital industrial gas widely used in the oil refining and chemical industries; it can also serve as a clean energy source for transportation. The U.S. Department of Energy (DOE) estimated the U.S. H_2 demand as high as 20–50 million metric tons per year by 2050, given the enormous need for clean energy to decarbonize industry, transportation, and the power grid [5]. Currently, ~95% of H_2 production in the United States uses fossil fuel reforming (e.g., petroleum, natural gas, and coal) [6]. Reforming plastic waste with improved performance and reductions in capital and operating costs to achieve H_2 production at less than $1/kg is targeted to reduce fossil fuel demand for clean H_2 production and address the worldwide challenges of rapidly growing plastic waste [5,6].

Over the past three decades, large-scale recycling strategies for repurposing plastics have been implemented across Western countries. However, as of 2023, only approximately 8.8% of collected plastics undergo mechanical or chemical recycling on a global scale [4,7] (Figure 1). In the United States, plastics constitute 12.2% of municipal solid waste, with only 4.47% being effectively recycled [8]. Additionally, plastic upcycling is a concept where waste plastic serves as a feedstock for the synthesis of value-added products, including advanced polymers, functional molecules, and high-performance materials (Figure 2). This approach is considered complementary to both chemical and mechanical recycling, as it enhances resource efficiency by transforming waste plastics into higher-value applications.

Photoreforming is considered a potentially sustainable and environmentally friendly process for upcycling plastic waste or as a tertiary recycling method [9–12]. Photoreforming has the potential to convert plastic waste into value-added chemicals while simultaneously generating H_2 using plastic-derived organics as sacrificial agents. This approach not only supports waste valorization but also reduces greenhouse gas (GHG) emissions, contributing to carbon-neutral, sustainable energy systems [13]. Compared to traditional water splitting, photoreforming offers advantages such as lower energy requirements and the added benefit of utilizing waste streams [12,14]. Key factors influencing photoreforming efficiency include the design of photocatalysts, reaction conditions, and system configurations [15]. Strategies to enhance catalytic performance involve improving light absorption, charge carrier separation, and surface reaction rates [15]. Recent research has focused on optimizing photooxidation pathways to enhance product selectivity through strategic catalyst modifications, advanced characterization techniques, computational modeling, and the refinement of process conditions and reactor design [16]. Future advancements in photoreforming technology may involve holistic approaches combining catalyst and system designs, advanced characterization techniques, and artificial intelligence to establish structure-mechanism-function relationships [16].

 doi:10.20944/preprints202504.1506.v1

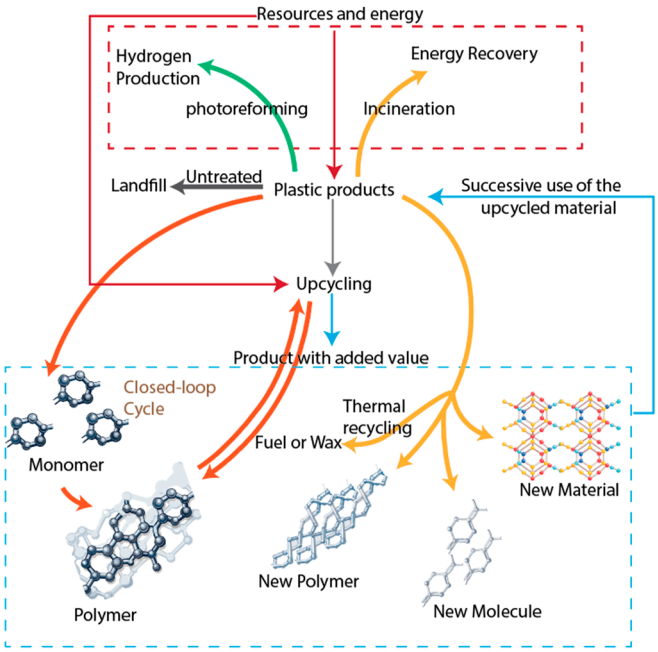

Figure 2. Plastic upcycling to synthesize new polymers, molecules, and materials.

Photoreforming of plastic waste provides a sustainable pathway for H_2 production [17–20]. Research on plastic photoreforming for H_2 production reveals several critical gaps that must be addressed to improve efficiency and scalability. These challenges primarily concern the optimization of photocatalysts, a deeper understanding of reaction mechanisms, and the effective integration of byproducts into the H_2 production and/or plastic manufacturing process. Further investigation is needed to elucidate the kinetics of photoreforming reactions, particularly under varying environmental conditions and plastic compositions.

This review critically examines the fundamentals of plastic photoreforming, including the range of plastic waste that can serve as sacrificial agents and the impact of pretreatment and post-treatment strategies on H_2 yield. A comprehensive analysis of various photocatalysts used in photoreforming is presented, with a focus on catalyst engineering, composite material development, characterization techniques, and advanced design and fabrication methods. Additionally, the formation of byproducts and the potential for extracting value-added products are explored as opportunities to enhance the process. Finally, the study assesses the lifecycle and technoeconomic aspects of plastic waste photoreforming, providing an integrated perspective on its environmental and societal implications for sustainable H_2 production.

2. Fundamentals of Plastic Photoreforming

2.1. Overview of Photoreforming

The photocatalytic conversion of plastic waste can be carried out using either heterogeneous semiconductor or homogeneous solution catalytic systems. In the heterogeneous photoreforming process, the catalyst absorbs photons from a radiation source, resulting in the excitation of electrons (e^-) from the valence band (VB) to the conduction band (CB) while simultaneously generating photogenerated holes (h^+). These charge carriers (e^- and h^+) migrate to the catalyst surface, facilitating both H_2 production and plastic degradation. Plastic waste undergoes oxidation by the photogenerated holes, leading to the formation of various organic molecules. Concurrently, the excited electrons participate in the reduction of water, yielding molecular H_2 [17]. Homogeneous photocatalysis occurs when both the catalyst and reactants exist in the same phase. In this process, light activates the catalyst, triggering chemical reactions. The sequence unfolds as follows:

 doi:10.20944/preprints202504.1506.v1

- The catalyst absorbs photons, exciting electrons from the highest occupied molecular orbital to the lowest unoccupied molecular orbital, resulting in an activated catalyst.
- The excited catalyst interacts with reactants, generating active intermediates through H_2 atom transfer or electron transfer, thereby selectively facilitating plastic conversion.

Efficient photocatalysts should possess a narrow bandgap, broad light absorption capability, low electron-hole recombination rates, better separation and transfer of photogenerated charge carriers, and structural stability over multiple reaction cycles [21,22]. Bandgap engineering, surface modification, and heterojunction construction are design strategies for high-performance catalysts [23–26]. Bandgap engineering modifies the electronic properties of photocatalysts to optimize light absorption and charge transfer, thereby enhancing their photocatalytic performance. By tailoring the bandgap, the photocatalyst's ability to harness solar energy improves, increasing its effectiveness in driving the photoreforming process. For example, the design of bifunctional $Mn_xCd_{1-x}S$ photocatalysts allows for bandgap tuning by adjusting the Mn/Cd ratio, facilitating the conversion of xylose into valuable C3 organic acids and H_2 [27]. Similarly, donor-acceptor conjugated microporous polymers (CMPs) achieve tunable bandgaps by varying the 9-fluorenone content, while incorporating acetylenic linkages into 2D heterotriangulene polymers effectively reduces the bandgap [28,29]. Deposition of co-catalysts, metal oxides, sulfides, nitrides, phosphides, and carbides (MoO_x, CoO_x, MoS_2, NiS_2, transition metal nitrides, CoP_2) [30–32], noble metals (Au, Pt, Pd, Rh, Ru, Ir, Ag) [33,34], metal-free catalysts (Carbon nitride) [35,36], multicomponent metal oxides (Co, Mg, Ni, Cu, Zn)$_{1-x}Ca_xO$ [37], single-atom deposition [38] and 2D semiconductor materials can refer to the bandgap engineering strategies to enhance the catalytic efficiency [39]. The current trends and performance of these catalysts and their composites are further discussed in Section 4.

Plastic photoreforming is influenced by several critical factors that determine its efficiency and product yield. The choice of photocatalyst is paramount, and optimizing the concentration of photocatalysts in reaction suspensions can enhance H_2 production efficiency [17,19]. Additionally, the molecular structure of plastic has a significant impact on the photoreforming process. Different polymers exhibit varying degrees of susceptibility to photodegradation and conversion efficiency [40]. Factors such as reaction temperature, pH, reactor design, solvent effects, and light intensity are critical for enhancing the plastic photoreforming process [17].

2.2. Reaction Pathways and Mechanisms

The polymer degradation pathways are mainly based on the type of polymer, and the depolymerization mechanism involves a series of hydrogen atom transfer, single electron transfer, and oxygen atom transfer events enabled by the excited state of a catalyst [41]. Two main groups of plastics are considered when discussing degradation pathways: those with a carbon backbone and those with heteroatoms in the main chain. The degradation of polymers with a carbon-carbon backbone is initiated by factors such as UV-radiation and oxygen, leading to chain scission, forming smaller polymer fragments [42]. The most susceptible degradation pathway for carbon backbone structures, such as polyethylene (PE), polypropylene (PP), and polystyrene (PS), is photo-initiated oxidative degradation. Initiation, propagation, and termination are the three main steps of the degradation mechanism. The chemical bonds in the main polymer chain are broken by light or heat, and free radicals are formed during the initiation step. Unsaturated chromophore groups absorb light energy, driving the initiation process. However, polymers such as PE and PP are resistant to photo-initiated degradation due to the absence of unsaturated double bonds in their carbon backbone. The free radicals formed during the initiation step react with oxygen, resulting in the formation of a peroxyl radical in the propagation step. The subsequent complex radical reactions, which form autoxidation, ultimately lead to chain scission or crosslinking. Termination occurs when two free radicals combine to form inert products. Random chain scission, end chain scission, branching, crosslinking, and the formation of oxygen-containing functional groups are the results of oxidation degradation [43,44]. Aldehydes, ketones, and olefins are the expected final products of the

 doi:10.20944/preprints202504.1506.v1

degradation. Furthermore, the reduction in molecular weight and subsequent brittleness increase the surface area available for propagating the reactions.

Photo-oxidation, biodegradation, and hydrolytic degradation are relevant pathways for polymers containing carbon and heteroatoms in the main chain, such as polyethylene terephthalate (PET) and polyurethane (PU). Photodegradation of PET cleaves the ester bond, forming a carboxylic acid end group and a vinyl end group directly or forms radicals, which eventually transform into carboxylic acid end groups [45]. Chain scission is the primary result of photo-oxidation, and the formed carboxylic acid end groups promote thermal and photo-oxidative degradation.

PET is susceptible to hydrolytic degradation, which is the primary mechanism of low-temperature degradation. Carboxylic acid and alcohol functional groups are formed during the hydrolysis process. Hydrolysis of PET is an autocatalytic reaction, whereas the rate of hydrolysis is higher under acidic or basic conditions [46,47]. PET hydrolyzed into terephthalate, ethylene glycol, and isophthalate in an alkaline aqueous solution and further photoconverted to formate, glycolate, ethanol, acetate, and lactate over photocatalysts (such as CdS/CdO_x quantum dots, Pt/TiO_2) under mild conditions [48–50].

2.3. Thermodynamic and Kinetic Considerations

From a thermodynamic perspective, overall water splitting, which involves both proton reduction and water oxidation, requires an energy input exceeding the Gibbs free energy (ΔG) of +237 kJ/mol. This high energy demand arises because water splitting is a highly endothermic process, necessitating substantial energy to break the strong O–H (~460 kJ/mol) bonds in water molecules to generate H_2 and oxygen. Consequently, the thermodynamic barrier for water splitting is substantial, necessitating considerable free energy input, rendering the process inherently unfavorable. In contrast, plastic photoreforming offers distinct thermodynamic advantages. Another critical factor influencing reaction rates is the activation energy, which reactants must overcome to form products. In photocatalytic water splitting, the primary challenge is the oxidation of water to oxygen, which is hindered by its high activation energy. This reaction demands high-energy photons and involves complex electron transfer mechanisms and molecular reorganization, making it kinetically difficult. On the other hand, plastic oxidation reactions during photoreforming exhibit lower activation energy, particularly in cases where small molecule degradation occurs. The C–C (~350 kJ/mol) and C–H (~410 kJ/mol) bonds in plastic macromolecular chains are more readily broken by reactive oxygen species generated by photocatalysts. Additionally, oxidation products, such as small organic molecules, are easier to form compared to oxygen, further reducing kinetic barriers. As a result, incorporating waste polymers into chemical and energy production systems presents a promising strategy for advancing sustainable energy and resource recovery [51].

Plastic photoreforming offers thermodynamic benefits for H_2 generation compared to direct water splitting. Pre-treating plastics enhances interactions with the catalyst, enabling them to function as photogenerated hole scavengers. This reduces charge recombination, enhances proton reduction, and ultimately increases H_2 production. The H_2 production mechanism in plastic photoreforming closely resembles conventional photocatalytic H_2 evolution using organic sacrificial agents. From a thermodynamic perspective, the photocatalyst's CB must be positioned above the reduction potential of H_2, while its VB must be more positive than the oxidation potential of the plastic substrate. Plastic photoreforming presents a sustainable approach for both H_2 production and plastic waste reduction, offering a promising solution for solar energy storage [16,52,53].

3. Types of Plastics and Their Suitability for Photoreforming

3.1. Common Plastics

Polylactic acid (PLA), PET, PP, PE, PS, and polyvinyl chloride (PVC) are among the most widely used plastics, and their suitability for photoreforming varies depending on their chemical structure and degradation pathways (Figure 3). PET is considered one of the most favorable candidates due to

 doi:10.20944/preprints202504.1506.v1

its ester functional groups, which are susceptible to hydrolysis and oxidation under photocatalytic conditions [15]. Studies have demonstrated that PET photoreforming in alkaline media, particularly with carbon nitride-based photocatalysts, leads to the effective breakdown of the polymer into terephthalic acid (TPA) and ethylene glycol (EG), which can subsequently undergo further oxidation to generate H_2 and value-added chemicals (Figure 3). PP and PE (both high- and low-density PE) present more significant challenges due to their highly stable hydrocarbon backbones, which lack functional groups that facilitate photocatalytic attack. However, recent research has shown that pre-treatment methods, such as soaking in alkaline solutions or mild thermal activation, can enhance their degradation rates, making them more amenable to photoreforming [54].

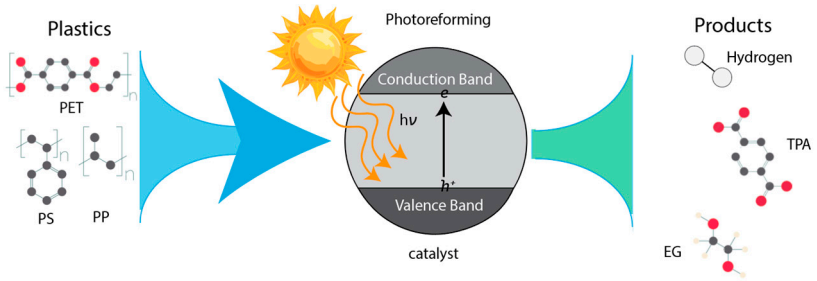

Figure 3. Photoreforming of plastics for H2 and valuable chemical production.

PS and PVC exhibit distinct behaviors in photoreforming applications. PS, an aromatic polymer, tends to generate benzene-derived oxidation products such as benzoic acid, making its conversion pathways different from those of aliphatic plastics [54]. This distinct degradation behavior suggests that catalyst design should be tailored to aromatic systems when targeting PS. PVC, while structurally similar to polyolefins, poses additional challenges due to its chlorine content [15]. The release of chlorine radicals or hydrochloric acid during degradation can corrode catalysts and form toxic byproducts, necessitating careful process control and material selection. Despite these challenges, some studies have explored photocatalytic systems capable of selectively breaking C-Cl bonds while minimizing unwanted side reactions. Given these considerations, PET and PS emerge as more suitable candidates for photoreforming due to their inherent reactivity, while PP, PE, and PVC require additional modifications or processing steps to improve their conversion efficiency [55].

3.2. Characteristics Affecting Photoreforming

The presence of additives, fillers, and dyes in real-world plastic waste significantly influences the efficiency of photoreforming processes. Additives such as plasticizers, stabilizers, and flame retardants can alter the optical and electronic properties of plastics, potentially hindering light absorption and charge carrier generation during photoreforming. For instance, Uekert et al. demonstrated that additives in PET can act as recombination centers for photogenerated electrons and holes, reducing the overall photocatalytic activity [56]. Similarly, dyes and pigments in plastics can compete with photocatalysts for photon absorption, leading to lower photoreforming efficiency [55]. These components often introduce complexities in the photoreforming process, as their chemical stability and interaction with photocatalysts vary widely [57].

Moreover, fillers such as calcium carbonate or silica, commonly added to plastics to improve mechanical properties, can also impact photoreforming [58,59]. These materials may scatter light or create physical barriers that reduce the accessibility of the plastic surface to photocatalysts. Previous findings highlighted that the presence of fillers in PP decreased the effective surface area available for photocatalytic reactions, thereby lowering the H_2 production rate during photoreforming [60,61]. To address these challenges, researchers have emphasized the need for tailored photocatalytic systems that can accommodate the heterogeneous nature of real-world plastic waste, ensuring efficient light utilization and charge transfer despite the presence of additives and fillers.

 doi:10.20944/preprints202504.1506.v1

The surface area, crystallinity, and molecular weight of plastics are critical factors that determine their photoreforming efficiency [62]. A higher surface area generally enhances the interaction between the plastic and the photocatalyst, facilitating better light absorption and charge transfer. Additionally, mechanically ground PET with increased surface area exhibited higher H_2 evolution rates during photoreforming compared to untreated PET [56]. This is attributed to the greater exposure of reactive sites and improved contact with the photocatalyst. However, the crystallinity of the plastic also plays a significant role; highly crystalline regions are often more resistant to photocatalytic degradation due to their dense molecular packing and lower accessibility [63]. Molecular weight is another key factor influencing photoreforming. High molecular weight polymers typically have longer chains and stronger intermolecular forces, making them more challenging to degrade. A study by Nguyen et al. found that low molecular weight polyethylene was more readily photoreformed than high molecular weight polyethylene, as the shorter chains were easier to break down into smaller intermediates [64]. Similarly, the molecular weight of polyethylene significantly affects its photoreforming efficiency, with lower molecular weight polymers showing higher H_2 production rates [65]. These findings underscore the importance of considering the structural properties of plastics when designing photoreforming systems, as optimizing surface area, crystallinity, and molecular weight can significantly enhance the overall efficiency of the process.

Pre-treatment strategies, such as grinding and thermal treatment, are essential for enhancing the photoreactivity of plastic waste [54,66]. Grinding plastic into smaller particles increases the surface area, thereby improving the contact between the plastic and the photocatalyst. This mechanical pre-treatment also disrupts the polymer matrix, making it more susceptible to photocatalytic degradation. For instance, a study demonstrated that reducing the particle size of biomass substrates increased the specific surface area and number of active sites, resulting in improved H_2 production efficiency during photoreforming [67]. The increased surface area and reduced particle size facilitated more efficient light absorption and charge transfer, leading to enhanced photoreforming performance.

Thermal pre-treatment is another effective strategy to improve the photoreactivity of plastics. Heating plastics to temperatures below their melting point can reduce crystallinity and introduce defects in the polymer structure, making them more amenable to photocatalytic degradation [68]. Novel findings have illuminated that thermally pre-treated PS had a lower crystallinity and higher photoreforming efficiency compared to untreated PS [69]. The thermal treatment disrupted the polymer chains, creating more reactive sites for photocatalytic attack. Additionally, combined mechanical and thermal pretreatment methods significantly enhance photoreforming efficiency by simultaneously increasing surface area and reducing polymer crystallinity [17]. Mechanical treatments, such as grinding or milling, reduce particle sizes, improving catalyst-substrate interaction, while thermal methods decrease crystallinity, making polymer chains more accessible for catalytic degradation [70]. These pre-treatment strategies highlight the importance of modifying the physical and chemical properties of plastics to optimize their photoreforming potential, paving the way for more efficient and sustainable waste-to-energy conversion technologies.

4. Photocatalysts and Catalyst Engineering

4.1. Semiconductor Photocatalysts

Semiconductor photocatalysts are the key component of plastic photoreforming systems due to their ability to convert photon energy into redox reactions that degrade plastic waste and simultaneously generate H_2. This process of converting solar energy to chemical energy relies on the bandgap of the photocatalysts, which designate the wavelength of light it can absorb, thereby influencing photoreforming efficiency. In the reason studies, various strategies—such as bandgap tuning, doping, and surface modification—have been studied to enhance the visible-light response and stability of these catalysts under real operating conditions [18,71,72]. These findings underscore the importance of selecting semiconductors that can effectively harvest sunlight, particularly in the

 doi:10.20944/preprints202504.1506.v1

visible spectrum, to enhance the overall process's economic and environmental viability. The primary objective of customizing the bandgap to visible light is that most solar radiation falls within the visible region, thereby maximizing photon utilization and significantly improving the overall solar-to-hydrogen conversion efficiency (Figure 4A).

In addition to bandgap engineering, chemical and thermal stability are significantly important due to impurities and harsh light irradiation conditions. During plastic photoreforming, partially degraded polymer fragments, dyes, and other additives can produce reactive intermediates (e.g., radicals or small organics), potentially deactivating the catalyst through fouling or chemical attack. Consequently, researchers emphasize developing robust semiconductors that can withstand harsh oxidative environments without significant structural or compositional changes [73]. Additional, high surface area and advantageous morphology (e.g., nanostructured or porous architectures) further boost the contact between catalysts and plastic-derived intermediates, enhancing reaction rates [74]. Among conventional photocatalysts, Figure 4B illustrates that the catalysts fulfill the bandgap requirement to undergo H_2 production via photoreforming. TiO_2 remains a leading candidate due to its low cost, non-toxicity, and strong oxidation potential. However, its wide bandgap (~3.0-3.2 eV) limits absorption primarily to UV light, which constitutes only a small fraction of the solar spectrum [10]. Similarly, ZnO exhibits high activity under UV irradiation; however, its susceptibility to photocorrosion under certain conditions can reduce its long-term stability in plastic degradation reactions [75,76]. Meanwhile, narrower-bandgap semiconductors such as CdS (2.4 eV) show promise for visible-light photoreforming, though cadmium toxicity and photocorrosion concerns have motivated researchers to develop protective layers or co-catalysts that stabilize CdS during prolonged operation [10,77].

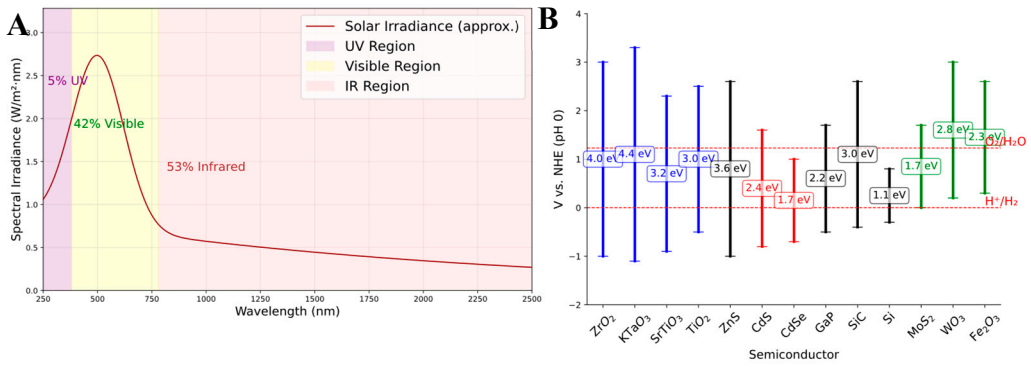

Figure 4. (**A**) Solar spectrum from 240 nm to 2500 nm wavelengths obtained from Ref.[78] (**B**) The bandgap energy of photocatalysis, as determined from the data obtained in Ref.[79].

4.2. Metal-Organic Frameworks (MOFs) and Carbon-Based Composites

One effective strategy for tuning the bandgap involves introducing foreign compounds into the photocatalyst, thereby forming composite materials that alter its electronic structure. This approach can enhance light absorption, improve charge carrier dynamics, and ultimately boost photocatalytic performance compared to unmodified semiconductors. The MOF-derived photocatalysts are one of these strategies that are utilized for solar H_2 generation and pollutant degradation. MOFs can facilitate charge separation by creating internal junctions or built-in electric fields through innovative synthesis and structural design [80]. These modifications enhance the directional flow of charge carriers, reducing recombination losses and improving photocatalytic efficiency. For instance, inducing band bending in a Ti-based MOF established an internal electric field that boosted H_2 evolution rates by over an order of magnitude (up to 56× higher than the pristine MOF) [81]. MOF-derived composites also exhibit improved stability and reactivity in pollutant removal. Strong interfacial bonds in MOF heterostructures (e.g., Fe–O–P linkages) can act as “electron highways,”

 doi:10.20944/preprints202504.1506.v1

accelerating charge transfer for faster contaminant breakdown [80]. Furthermore, transforming MOFs into porous carbon frameworks has yielded durable, high-performance photocatalysts; for example, a bimetallic Ni/Co–N–C derived from MOFs achieved ~100% dye degradation in 60 minutes and maintained its efficiency over multiple reuse cycles [82].

Expanding on these advancements, MOF-derived photocatalysts have illustrated great promise in plastic photoreforming, where these materials facilitate both plastic degradation and H_2 evolution under visible-light irradiation. Recent studies highlight the effectiveness of ZnO/UiO-66-NH_2 composites, where the MOF scaffold stabilizes ultra-small ZnO nanocrystals, forming a heterojunction that promotes charge transfer and enables efficient conversion of PLA and PVC plastics into acetic acid (~91% selectivity) while concurrently generating H_2 [83]. Similarly, defect-engineered CdS-based MOFs have demonstrated a 23-fold increase in H_2 production compared to conventional CdS, attributed to sulfur vacancies that enhance active sites and suppress charge recombination [84]. These approaches, ranging from doping-induced band engineering to hybrid nanostructures, significantly enhance charge-carrier separation, stability, and overall photoreforming efficiency in both water-splitting and plastic degradation applications.

Similar performances have been observed with g-C_3N_4/graphene-based photocatalysts, which leverage graphene's conductivity and stability to upgrade the performance of graphitic carbon nitride. Incorporating graphene (or its derivatives, such as reduced graphene oxide (rGO)) creates a conductive network that traps electrons and inhibits electron–hole recombination, thereby extending charge-carrier lifetimes and enhancing light absorption [72]. As a result, g-C_3N_4/graphene hybrids illustrate enhanced activity in H_2 evolution and organic pollutant oxidation under visible light. Previous studies have demonstrated that adding a fraction of rGO to g-C_3N_4 tripled the photocatalytic degradation rate of bisphenol A (achieving ~99% removal in 1 hour) by enhancing electrical conductivity and facilitating the separation of charge carriers [85]. Novel architectures, such as three-dimensional g-C_3N_4-graphene aerogels, further enhance charge transport and robustness. Protonating g-C_3N_4 to assemble it onto graphene yields a strong interfacial electric field and intimate contact, which significantly facilitates photogenerated charge transfer.

Building on these advancements, g-C_3N_4 graphene-based photocatalysts have emerged as highly effective materials for the photoreforming of plastics. Recent studies demonstrate that B-doped g-C_3N_4 nanotubes exhibit remarkable photocatalytic efficiency in plastic reforming, achieving an H_2 evolution rate of 3240 $\mu molg^{-1}h^{-1}$ from PET plastic, a performance that surpasses many traditional metal-based catalysts [86]. Similarly, a ternary NiCoP/rGO/g-C_3N_4 composite has been shown to achieve 3.6× higher H_2 production than conventional NiCoP/g-C_3N_4 systems, with an apparent quantum efficiency of 1.7% at 420 nm, owing to the synergistic role of rGO as an electron mediator and NiCoP as an active catalytic site [87]. These architectures not only promote efficient charge-carrier separation but also enable selective oxidation of plastic into valuable intermediates such as formate and acetate. Furthermore, 2D/2D Z-scheme heterojunctions combining g-C_3N_4 and graphene-modified C_3N_5 have demonstrated enhanced light-harvesting capabilities and higher H2 evolution rates under visible light [88]. These findings confirm that g-C_3N_4/graphene-based materials provide a sustainable and efficient platform for plastic photoreforming, integrating low-cost, metal-free catalytic systems with high activity and long-term stability.

4.3. Noble Metal and Transition Metal Co-catalysts

Noble metals such as platinum (Pt), palladium (Pd), and gold (Au) are highly effective co-catalysts for photocatalytic H_2 production. Their effectiveness stems from a combination of electronic properties and surface chemistry [89]. The noble metals have high work functions and form Schottky barriers at the semiconductor interface, causing the electrons to trap from the photocatalyst and prevent electron-hole recombination (Figure 5) [90,91]. Trapped electrons accumulate on the metal nanoparticles, where they reduce water (or protons) to H_2 gas. Meanwhile, the photogenerated holes remain on the semiconductor to oxidize the plastic substrate subsequently. In essence, noble metal co-catalysts act as electron sinks and H_2 evolution sites, which can boost H_2 production rates by orders

 doi:10.20944/preprints202504.1506.v1

of magnitude even at petite loadings (typically 1–3 wt%) [66]. For example, Pt is widely regarded as an ideal H_2-evolution co-catalyst due to its optimal hydrogen binding energy and has historically shown the highest activity among metals [92]. Similarly, Pd and Au nanoparticles also enhance H_2 generation, though conventional activity rankings for nanoparticle co-catalysts follow Pt > Pd > Au in most cases [93]. Therefore, noble metals play a crucial role in enhancing charge separation and providing abundant active sites for the H_2 evolution reaction. In summary, the noble metal co-catalysts should undergo different key roles in H_2 evolution [90]. The mechanisms involve electron trapping where High-work-function metals (Pt, Pd, Au) form junctions that siphon electrons from the semiconductor, reducing recombination. The metal surfaces provide active sites for H_2 to catalyze proton reduction to H_2 efficiently, lowering the energy barrier for H_2 evolution. Adding a small amount of Pt or Au can also increase H_2 generation rates by several orders of magnitude compared to the bare photocatalyst. In some cases, Au nanoparticles can also exhibit localized surface plasmon resonance under visible light, enhancing light absorption and hot-electron injection, though their primary function in photoreforming remains as electron traps and catalytic sites.

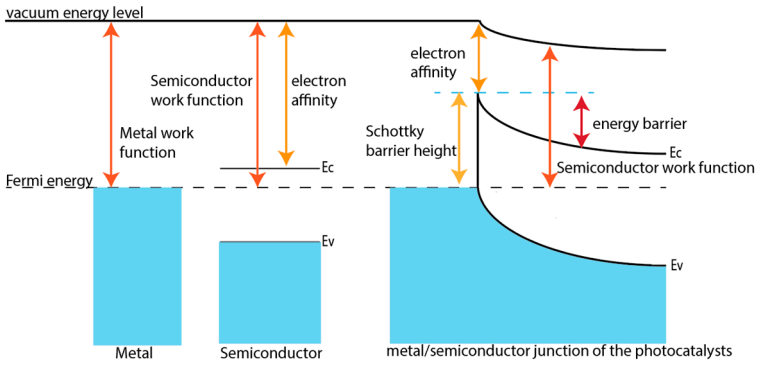

Figure 5. A Schottky barrier is created when a metal with a higher work function forms a junction with a semiconductor, leading to electron transfer from the semiconductor to the metal and the formation of a depletion region that influences charge carrier dynamics [91]. The Ec and Ev are the conduction band and valence band, respectively, relative to the vacuum energy level.

These enhanced photocatalysts are utilized in plastic photoreforming and have advanced across a range of catalyst systems, extending beyond traditional noble-metal co-catalysts. Noble metal-based photocatalysts, namely Pt-loaded semiconductors, remain benchmark systems for high H_2 yields; however, transition metal and earth-abundant co-catalysts have rapidly gained prominence as cost-effective alternatives [56]. For example, nickel phosphide on carbon nitride (Ni_2P/CN) can promote efficient charge separation and H_2 evolution, matching or even surpassing Pt-based catalysts while maintaining multi-day stability. Meanwhile, hybrid catalyst designs (e.g., heterojunctions of CdS with MoS_2) have delivered enhanced H_2 generation and more controlled plastic oxidation, as the intimate semiconductor – cocatalyst interface boosts electron– hole separation and drives selective degradation toward value-added products [94]. These innovations collectively enhance charge-carrier separation, catalyst durability, and overall conversion efficiency, thereby narrowing the performance gap between noble-metal systems and sustainable, earth-abundant catalysts.

However, the reliance on precious metals poses economic and environmental challenges. Pt, Pd, and Au are expensive and have low crustal abundance, which limits scalability [90]. To address this, recent studies explore earth-abundant co-catalysts based on nickel (Ni), cobalt (Co), iron (Fe), and related compounds [95]. These cost-effective metals can mimic many of the charge-separation and catalytic functions of noble metals, although often with careful engineering to overcome their lower intrinsic activity [56]. For instance, nickel-based co-catalysts illustrate a high work function and form Schottky-like junctions with semiconductors. In fact, Ni-based nanoparticles and compounds, such as Ni_2P, have shown remarkable success in plastic photoreforming. A carbon nitride/Ni_2P system was demonstrated as a noble-metal-free photocatalyst for reforming PET plastic waste under visible light . Beyond Ni, researchers are investigating Co and Fe-based co-catalysts for photocatalysis. Cobalt

 doi:10.20944/preprints202504.1506.v1

compounds (e.g., cobalt phosphide or cobalt oxide) can also serve as sites for H_2 evolution; however, they are less common in plastic reforming studies, as these catalysts exhibit activity in analogous biomass photoreforming systems [96]. Iron-based catalysts are attractive due to iron's low cost and benign nature. Nevertheless, Fe often requires structuring (such as forming bimetallic alloys or doping into other materials) to be effective for H_2 evolution because pure iron can corrode or deactivate under reaction conditions. A recent strategy to leverage multiple earth-abundant metals is the development of high-entropy oxides and oxynitrides that incorporate several elements, including Ni, Co, and Fe, among others, to tune the electronic structure and stability [97]. For instance, introducing nitrogen into a high-entropy oxide (containing Ti, Zr, Hf, Nb, and Ta) to create a high-entropy oxynitride achieves higher yields of H_2, formic acid, and acetic acid from PET plastic than the noble-metal-free oxide alone. The added nitrogen distorted the lattice and altered the local electronic environment of the metal cations, narrowing the band gap and suppressing electron-hole recombination. Overall, replacing noble metals with Ni-, Co-, or Fe-based co-catalysts is a major trend for improving the economic and environmental sustainability of plastic photoreforming catalysts.

The crucial question is how well these earth-abundant co-catalysts perform relative to traditional noble metals in photocatalytic plastic reforming. Comparative studies indicate that while noble metals still often lead in raw activity, certain non-noble formulations come surprisingly close or even match their performance under optimized conditions. A systematic investigation of various metal/TiO_2 photocatalysts for reforming biomass-derived substrates (a process analogous to plastic photoreforming) found that the H_2 evolution activity follows the order Pt > Cu ≈ Au >> Ag [98]. Copper co-catalysts in this study produced H_2 at rates only slightly lower than those of platinum and on par with gold, highlighting Cu as a realistic, low-cost alternative. Similarly, nickel-based co-catalysts have demonstrated competitive performance. In a recent visible-light PET photoreforming system, Ni_2P on g-C_3N_4 achieved an H_2 production rate of ~82.5 $\mu molh^{-1}g^{-1}$, slightly exceeding that of a Pt-loaded g-C_3N_4 benchmark (~72 $\mu molh^{-1}g^{-1}$ under the same conditions) [56]. In addition to comparable rates, the Ni_2P co-catalyst demonstrated superior stability, retaining its activity over 24 hours without loss, whereas the Pt catalyst suffered a notable decline over the same period. These findings demonstrate that, with proper design, non-noble co-catalysts can rival or surpass noble metals in plastic reforming systems. It is worth noting that the form and preparation of the co-catalyst can influence these comparisons [56]. Even within noble metals, morphology and dispersion matter: conventional nanoparticles follow the trend Pt > Pd > Au in H_2 evolution; yet, when dispersed as single atoms on TiO_2, the activity order flips to Pd > Pt > Au [93]. In its single-atom form, a Pd atom can utilize its d-electrons more effectively for proton reduction, outperforming even single-atom Pt under those specific conditions. This intriguing result suggests that the "best" co-catalyst can depend on numerous operational and synthesis conditions, thereby being subject to the runtime environment (Table 1). Overall, noble metals still set the benchmark for the highest activities, although transition metal co-catalysts (such as Ni and Cu) have significantly narrowed the gap. With continued innovation in catalyst architecture, many non-noble materials now achieve H_2 yields of the same order of magnitude as those of Pt-based systems, marking significant progress toward economically viable plastic-to-hydrogen conversion.

Table 1. Comparison of noble vs. non-noble co-catalysts for photocatalytic plastic reforming.

Category	Noble Metal Co-Catalysts (Pt, Pd, Au)	Non-Noble Metal Co-Catalysts (Ni, Co, Fe, Cu, Mo, etc.)
Hydrogen Evolution Efficiency	High activity, excellent electron trapping, and fast proton reduction.	Moderate to high activity dependent on material engineering (doping, alloying, or structuring).
Charge Separation	Forms Schottky junctions, effectively suppressing electron-hole recombination.	Requires heterojunctions or defect engineering to achieve similar charge separation efficiency.

 doi:10.20944/preprints202504.1506.v1

Stability and Durability	Chemically stable under reaction conditions, low corrosion rate.	Some non-noble metals (e.g., Fe) can corrode or deactivate over time unless properly stabilized.
Cost and Scalability	Very expensive and scarce, limiting large-scale applications.	Earth-abundant and low-cost, catalysts are highly scalable for industrial use.
Environmental Impact	Mining and refining noble metals have significant environmental impacts.	More sustainable, widely available, and eco-friendly.
Versatility	Effective across a range of photocatalytic systems (e.g., plastic reforming, water splitting).	Catalysts can be engineered into various alloys and oxides to enhance versatility and selectivity.
Activation Energy and Reaction Kinetics	Low activation energy, enabling rapid reaction kinetics.	Requires co-doping (e.g., Ni_2P, CoP, MoS_2) to reduce activation energy for HER.
Long-Term Performance	Maintains high catalytic performance over extended use.	Some non-noble metals may degrade or lose efficiency over prolonged cycles.
Engineering Potential	Limited modification potential due to intrinsic properties of noble metals.	High tunability is achieved through the capabilities of doping, alloying, or nanostructuring for enhanced photocatalytic properties.

4.4. Design and Fabrication Strategies

Recent studies have shifted focus toward innovating photocatalyst synthesis routes and architectures to boost activity intrinsically, complementing the use of noble-metal co-catalysts and MOF/carbon composites. The choice of synthesis method alone can significantly influence the phase, morphology, and surface properties of photocatalysts [99]. Sol–gel methods are one such approach that enables fine control over composition and heterojunction formation at the nanoscale. For example, a $NiTiO_3/TiO_2$ nanocomposite prepared via an optimized sol–gel route formed an intimate phase junction that broadened UV-visible absorption and reduced charge recombination by ~85%, yielding a 17% higher H_2 evolution rate than pristine $NiTiO_3$ [100]. Similarly, a novel ionic liquid-assisted sol–gel process was utilized to dope Ce and P on TiO_2, achieving visible-light-active nanoparticles (~6 nm, 166 m^2/g) with a narrowed bandgap and suppressed electron–hole recombination [101]. The resulting doped TiO_2 completely degraded organic dyes under visible light in under 60 min, demonstrating how sol–gel chemistry (with dopants or additives) can produce highly active photocatalysts for environmental remediation.

Hydrothermal techniques are equally pivotal for tailoring nanostructures. The technology often yields distinct crystal phases or exposed facets that differ from sol–gel products, thus altering photocatalytic behavior [102]. TiO_2 nanoparticles from sol–gel vs. hydrothermal synthesis showed opposite affinities toward charged dye pollutants: as-prepared sol–gel TiO_2 preferentially degraded anionic dyes (~90% of methyl orange in 2 h) over cationic dyes (~40% methylene blue), whereas hydrothermal TiO_2 showed the reverse trend (favoring cationic dye ~91%). Subsequent calcination at 400 °C could alter or enhance these preferences, underscoring that synthesis and post-treatment tune the surface chemistry for selective pollutant degradation. Hydrothermal methods are also known for producing well-crystallized semiconductors at relatively low temperatures, facilitating the creation of heterojunctions (e.g., in situ grown composites) that improve charge separation for photocatalytic H_2 production [103].

High-temperature synthesis approaches, such as calcination, flame spray pyrolysis, and MOF-derived pyrolysis, have demonstrated notable progress in producing defect-engineered and hierarchical photocatalysts. Thermal treatments generally increase crystallinity and can induce phase junctions or dopant activation, which enhances charge transport. For instance, flame spray pyrolysis

 doi:10.20944/preprints202504.1506.v1

(FSP) – a rapid high-temperature aerosol process – has been employed to create oxygen-vacancy-rich $SrTiO_{3-x}$ perovskites [104]. The anoxic FSP technique introduces abundant TiO_2 lattice vacancies, effectively narrowing the functional bandgap and extending light absorption into the visible range. Notably, this single-step flame method is industrially scalable to kilogram quantities, offering a route to mass-produce defect-engineered photocatalysts with enhanced solar energy harvesting capabilities. Post-annealing treatments of sol–gel or hydrothermal products similarly enhance photocatalytic activity by transforming amorphous precursors into active crystalline phases and optimizing interfaces [102]. Moreover, MOF-derived thermal synthesis has enabled the formation of complex multi-component architectures; a recent example is a hierarchical $Ag/Sr_6Bi_2O_{9-\alpha}$-Bi_2O_3 ternary photocatalyst obtained by calcining a bimetallic MOF template [105]. The MOF-derived material exhibits interfacial oxygen vacancies and a porous framework that facilitates multiple light absorption–reflection events, leading to enhanced visible-light removal of various antibiotics and dyes. These high-temperature fabrication strategies thus play a critical role in inducing the crystallinity, dopants, and defects necessary for superior photocatalytic performance.

Architectural design at the nano- and micro-scale is crucial for improving light absorption and charge separation in photocatalysts. Hierarchical and nanostructured materials, such as core–shell structures, hollow spheres, mesoporous networks, and 1D nanowire arrays, can significantly increase the optical path length and active surface area. Inspired by natural photosynthetic systems, studies have shown that leaf-like hierarchical structures maximize photon capture through light scattering, multi-angle propagation, and focusing effects [106]. In artificial photocatalysts, similar principles apply: constructing TiO_2 across zero-, one-, two-, and three-dimensional forms (quantum dots, nanorods/tubes, nanosheets, and 3D mesoporous or core–shell assemblies) has emerged as an effective strategy to boost solar-to-fuel conversion efficiency [106]. One remarkable finding is the SiO_2@TiO_2 core–shell "nanolens" structure fabricated by a Stöber sol–gel method. The dielectric SiO_2 core and TiO_2 shell act in concert to concentrate incident light (the "beam effect"), enabling stronger light absorption within the photocatalyst. This enhanced light-harvesting capability allowed for efficient H_2 evolution with a minimal loading of Au co-catalyst, as the intense local field around the core–shell effectively drives reactions even at low noble metal content. Such core–shell or hollow architectures also shorten charge transport pathways and can create built-in electric fields at interfaces, improving charge separation and suppressing recombination. Porous and multi-tier structures are similarly beneficial. A hierarchically porous carbon nitride (hCN) framework decorated with single-atom Fe sites, for instance, has recently demonstrated a tandem approach to plastic photoreforming: it catalyzes the breakdown of resilient waste plastics into organic intermediates and then photoreforms those into H_2 gas [107]. The Fe-doped hCN's high surface area and interconnected pore network facilitated the near-total conversion of ultrahigh molecular weight polyethylene into soluble organics, subsequently achieving H_2 evolution rates of ~42 μmol h^{-1} under light, outperforming most existing plastic photoreforming methods. This exemplifies how nano-architectured supports (in this case, porous g-C_3N_4) and atomic-scale active sites can synergistically enhance both pollutant degradation and H_2 production in a single system.

Overall, tailored synthesis and hierarchical design strategies have yielded significant performance improvements across various photocatalytic applications. Sol–gel and hydrothermal routes produce finely tuned compositions and interfaces that enhance photocatalytic H_2 generation and targeted pollutant oxidation, while high-temperature and templating methods impart the crystallinity and defect structures necessary for broad-spectrum light utilization [100,101,104,105]. These approaches significantly enhance photocatalytic efficiency in plastic conversion, H_2 evolution, and environmental remediation by improving light-harvesting and charge-management at the catalyst level. In tandem with noble metal co-catalysts and MOF/carbon composites, these advanced design and fabrication strategies are driving the development of next generation photocatalysts with unprecedented activity and selectivity.

 doi:10.20944/preprints202504.1506.v1

4.5. Catalyst Characterization Techniques

Catalyst characterization is a fundamental aspect of photoreforming research, as it provides critical insights into the structural, electronic, and surface properties of catalysts that influence their performance. A comprehensive understanding of these properties enables the rational design and optimization of catalysts for enhanced efficiency in photoreforming processes. Table 2 summarizes the key findings, advantages, and disadvantages of various catalyst characterization techniques commonly employed in photoreforming studies.

Table 2. Summary of catalyst characterization techniques in photoreforming.

Characterization Technique	Key Findings	Advantages	Limitation
X-ray Diffraction (XRD)	Determines the crystalline structure and phase composition of catalysts.	Identifies crystalline phases.	Limited to crystalline materials.
X-ray Absorption Spectroscopy (XAS)	Probes local electronic and structural environment of specific elements.	Elucidates oxidation states, coordination numbers, and bond distances.	Requires synchrotron radiation sources.
Electron Microscopy (SEM and TEM)	Provides high-resolution images of catalyst morphology and nanostructure.	Observes particle size, shape, and dispersion.	Sample preparation can be intricate.
Surface Area and Porosity Analysis (BET Method)	Assesses surface area and porosity of catalysts.	Determines the availability of active sites.	Assumes idealized models that may not fit all materials.
UV-Vis Diffuse Reflectance Spectroscopy (DRS)	Investigates optical properties and bandgap energies.	Assesses light absorption capabilities.	Interpretation can be challenging for complex materials.
Photoluminescence (PL) Spectroscopy	Measures recombination rate of photogenerated electron-hole pairs.	Indicates efficiency of charge separation.	PL signals can be weak and require sensitive detection.
Fourier-Transform Infrared (FTIR) Spectroscopy	Identifies functional groups and chemical bonds on catalyst surfaces.	Provides insights into surface modifications and interactions with reactants.	Surface sensitivity can be limited.
Raman Spectroscopy	Offers information about molecular vibrations and crystal structures.	Identifies structural defects and phase compositions.	Fluorescence interference can obscure Raman signals.
X-ray Photoelectron Spectroscopy (XPS)	Provides information on elemental composition and chemical states of surface elements.	Surface-sensitive technique.	Limited to surface analysis (typically 1–10 nm depth).
Mass Spectrometry (MS)	Analyze reaction intermediates and products.	Offers insights into catalytic processes and efficiency.	Requires coupling with other techniques for comprehensive analysis.

 doi:10.20944/preprints202504.1506.v1

5. Reactor Configurations and Photoreforming Conditions

5.1. Bench-Scale Reactors and Scale-Up Challenges

Bench-scale systems serve as vital platforms for conducting foundational studies on photoreforming under tightly controlled conditions prior to pilot or commercial endeavors. There are mainly two primary reactor types that predominate: slurry reactors and fixed-bed (immobilized) reactors (Figure 6) [107]. Slurry reactors play a crucial role in photocatalytic processes by dispersing finely milled catalysts, such as TiO_2 nanoparticles, throughout the reaction fluid. This configuration significantly increases the catalytic surface area available for reactions, enhancing both mass transfer efficiency and photon absorption, which are essential for achieving high degradation rates and selectivity in pollutant removal. The dynamic nature of slurry reactors ensures that reactants continuously interact with active catalyst sites, thereby minimizing mass transfer limitations commonly encountered in immobilized systems. Furthermore, studies have demonstrated that slurry-type photoreactors exhibit higher reaction rates due to the uniform catalyst distribution compared to fixed-bed configurations [108]. However, a significant challenge in slurry reactors is the separation of fine catalyst particles from the treated effluent, which can hinder their industrial applicability. The size of the particles typically varies from nanometers to several micrometers during continuous reactor operation, with aggregation influenced by factors such as pH, ionic strength, and fluid dynamics. Traditional separation techniques, such as sedimentation or filtration, often struggle with nanosized catalysts due to their slow settling rates and the potential for clogging filters. Advanced solutions for addressing such challenges, including membrane photocatalytic reactors, have been developed to combine photocatalysis with membrane separation, effectively confining catalyst particles within the system while allowing treated water to pass through [108–110]. Research has shown that submerged polytetrafluoroethylene membranes with microfiltration properties can successfully retain TiO_2 particles within slurry reactors, maintaining consistent catalytic activity over extended operational periods. These advancements address the key limitations of catalyst recovery, paving the way for more sustainable and scalable slurry photoreactor applications.

In contrast, fixed-bed reactors immobilize catalysts onto structured media such as glass, metal meshes, or polymer supports, simplifying downstream catalyst handling, which is particularly important for repeated or continuous operations. However, the immobilized catalyst layers may experience diminished quantum efficiency if insufficient attention is given to coating thickness and uniformity, as thick or uneven coatings can restrict light transmission [111]. To address these challenges, researchers have explored various strategies, including the use of porous polymeric gels and membranes, which enhance catalyst performance by providing high surface areas and facilitating efficient mass transfer–features, particularly beneficial for continuous flow applications [112]. Additionally, immobilizing catalysts on stainless steel fleece has demonstrated improvements in shear strength resistance and mass transfer efficiency in rotating packed bed reactors, enhancing catalyst durability and performance under dynamic flow conditions. Through careful optimization of catalyst-coating techniques, reactor geometry, and flow configurations, attenuation effects can be mitigated, enabling long-term photoreforming experiments with minimal maintenance and material loss. Hence, the reactor configuration needs to be optimized to maintain the bench-scale photoreforming efficiency in a full-scale system.

 doi:10.20944/preprints202504.1506.v1

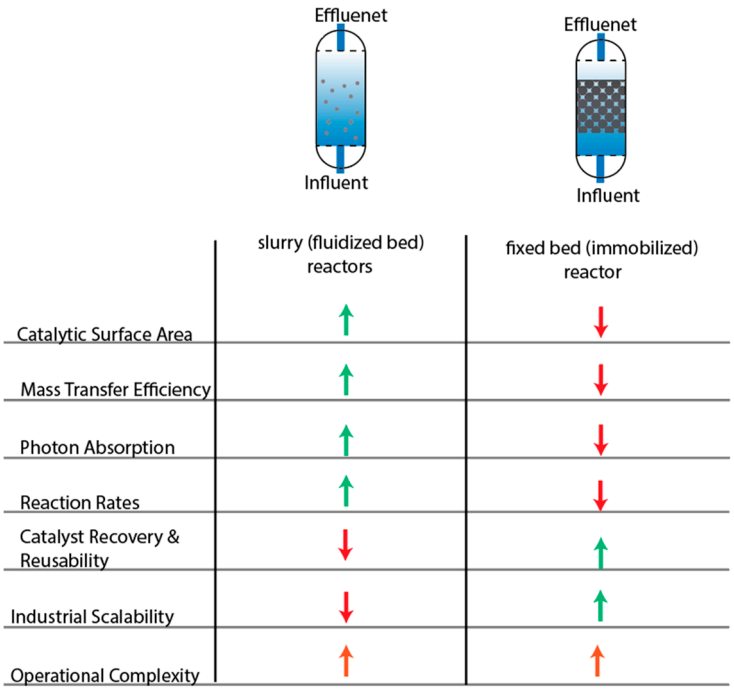

Figure 6. Comparison of slurry reactors and fixed-bed reactors based on their advantages and limitations.

5.2. Light Sources and Illumination Strategies

Selecting and deploying the appropriate light source is fundamental to optimizing photoreforming. Traditional TiO_2-based catalysts typically require UV-dominant sources, such as mercury lamps or UV LEDs, to induce electron-hole formation [16]. However, recent advances, including doped oxides and heterojunctions, target broader or visible regions of the solar spectrum, enhancing photon utilization efficiency and making solar-driven photoreforming more viable. Optimizing light delivery within photocatalytic reactors is crucial for enhancing photonic efficiency, which measures the proportion of absorbed photons that drive chemical transformations. Various illumination strategies have been implemented to improve light uniformity and maximize reactor performance, including immersion lamps, external LED panels, and compound parabolic collectors (CPCs) [113]. Immersion lamps provide direct and uniform illumination by submerging the light source within the reaction medium, minimizing losses due to light refraction at reactor walls. This configuration is particularly beneficial in high-volume photoreactors where achieving homogeneous irradiation is challenging. In contrast, LED panels offer advantages in terms of wavelength specificity, energy efficiency, and tunable intensity, making them a superior alternative to traditional UV lamps. Studies have shown that LED-based reactors outperform conventional UV lamp systems in terms of photonic efficiency and operational cost reductions when strategically placed to enhance photon penetration and reduce charge carrier recombination losses [113]. In addition to external LED configurations, innovative internal light delivery systems have emerged. For example, a recent study introduced a photocatalytic reactor that integrates modified strontium titanate onto side-emitting polymer optical fibers, enabling inside-out illumination. This configuration significantly improved photon confinement and surface activation, achieving up to seven-fold higher H_2 production compared to conventional PEC designs while also simplifying system architecture and reducing operational costs [114].

In solar-driven systems, CPCs significantly enhance photon flux by capturing and concentrating diffuse solar radiation onto the reactor surface. These collectors are particularly advantageous in CO_2 photoreduction and H_2 evolution reactions, ensuring prolonged illumination even under suboptimal solar conditions [115]. Beyond light source optimization, photoreactor design modifications also play a crucial role in improving photonic efficiency. Strategies such as using reflective coatings, transparent reactor windows, and structured catalyst supports have been shown to improve light

 doi:10.20944/preprints202504.1506.v1

distribution and utilization [116]. Optimizing reactor geometry to align photon penetration depth with catalyst placement minimizes photon loss and maximizes reaction efficiency, a principle validated through Monte Carlo ray tracing simulations. Additionally, advancements in bandgap-engineered photocatalysts and plasmonic nanostructures enable extended light absorption into the visible and near-infrared regions, enhancing solar spectrum utilization. Overall, improving photonic efficiency in photoreactors requires a multifaceted approach that integrates optimized light source placement, advanced reactor geometries, and innovative catalyst compositions. The research highlights the importance of integrating optical modeling with experimental validation to optimize light distribution and minimize energy losses. As photoreactor technologies evolve, the integration of hybrid LED-CPC systems and structured catalyst configurations presents a promising avenue for maximizing photon utilization in solar-driven photocatalytic processes.

5.3. Operational Parameters

Several interlinked operational parameters govern the success of photoreforming [66]. Temperature is frequently near ambient, but moderate heating (e.g., 40–60°C) can accelerate reaction kinetics, provided it does not trigger undesired thermal processes or degrade the catalyst [117]. Additionally, pH exerts a profound influence on photocatalytic reactions by modulating both the catalyst's surface charge and the speciation of dissolved organic molecules, thereby governing adsorption processes at the catalytic interface. The surface charge of semiconductor catalysts is determined by their point of zero charge (pHPZC), which dictates whether the surface is positively or negatively charged under varying pH conditions. When the solution pH is below the pHPZC, the catalyst surface carries a positive charge, favoring the adsorption of anionic species. Conversely, at pH levels above the pHPZC, the surface charge becomes negative, enhancing the adsorption of cationic species. This charge interaction is critical in facilitating or hindering pollutant degradation. A study on Ag/TiO_2 and α-Fe_2O_3/HY catalysts for organic pollutant degradation demonstrated that the highest degradation efficiencies occurred when the pH was lower than the pHPZC of the catalysts, suggesting that strong electrostatic interactions between the catalyst and the target pollutants enhanced the reaction rates [118]. Furthermore, pH influences the speciation of dissolved organics, altering their charge state and reactivity at the catalytic interface in photoreforming. For instance, weakly acidic or basic organic pollutants exhibit varying degrees of ionization depending on the surrounding pH, directly impacting their interaction with the catalyst surface [119]. Findings have illuminated that pH-dependent transformations in dissolved organic matter (DOM) affect its role as both a photosensitizer and an antioxidant, thereby modulating its overall impact on photodegradation processes. The study found that at higher pH values, the inhibitory effects of DOM on pollutant phototransformation increased, primarily due to changes in radical formation dynamics and antioxidant activity [120]. Furthermore, variations in pH alter the formation of hydroxyl radicals (•OH) and other reactive oxygen species (ROS), which play a key role in pollutant oxidation. Similarly, TiO_2 nanoparticles synthesized at different pH conditions exhibited distinct variations in surface charge and particle size, directly influencing their photocatalytic performance [119]. By leveraging the interplay between catalyst surface properties, pollutant speciation, and the generation of ROS, researchers can design more effective and robust photocatalytic systems tailored to specific environmental and industrial applications.

Flow conditions also play a role in determining the performance of photocatalytic reactors, particularly in continuous-flow systems where residence time dictates the interaction between photons, substrates, and catalysts. Optimizing flow rates is crucial for achieving a balance between photon absorption and mass transfer efficiency. If the flow rate is too high, reactants may pass through the illuminated zone too quickly, limiting their exposure to photocatalytic surfaces and reducing degradation efficiency. Conversely, if the flow rate is too low, reactants may become depleted in localized areas, leading to inefficient electron-hole interactions and decreased reaction rates [121]. Recent studies on continuous-flow photocatalytic reactors have demonstrated that maintaining a moderate flow rate prevents mass transfer limitations while ensuring that reactants

 doi:10.20944/preprints202504.1506.v1

remain within the active reaction zone for an adequate duration [122]. Additionally, simulations of light distribution in solar photocatalytic bubble column reactors highlight that variations in flow conditions significantly impact the local volumetric rate of energy absorption, reinforcing the importance of flow rate optimization for efficient reactor operation [123]. Beyond flow conditions, catalyst loading and substrate concentration must also be carefully optimized to prevent inefficiencies in light penetration and reaction kinetics. Excessive catalyst loading can lead to light scattering and shadowing effects, thereby reducing overall photonic efficiency [124]. In a photochemical rotor-stator spinning disk reactor study, researchers observed that increasing catalyst concentration initially improved degradation efficiency, but beyond an optimal threshold, excess catalyst particles obstructed light penetration, leading to diminished performance [121]. Similarly, substrate concentration must be controlled to avoid saturation of the catalytic surface, which can slow reaction kinetics and hinder the formation of ROS. Findings of photocatalytic fiber reactors have shown that high substrate concentrations can overshadow reaction dynamics, making it essential to strike a balance between reactant availability and catalyst accessibility [122].

Achieving an optimal balance among flow rate, catalyst loading, and substrate concentration is key to maximizing photon utilization and ensuring reactor stability. Studies on continuous-flow photocatalytic reactors for pollutant degradation suggest that fine-tuning these parameters leads to significant improvements in mineralization rates while maintaining catalyst efficiency. Additionally, computational fluid dynamics (CFD) simulations have been instrumental in modeling reactor performance under different flow conditions, offering valuable insights for the design of high-efficiency, scalable photocatalytic systems [124]. By integrating experimental findings with simulation models, researchers can develop advanced photoreactors that achieve superior reaction rates and long-term operational reliability. In general, optimizing the flow conditions, catalyst loading, and substrate concentration in continuous-flow photocatalytic reactors is essential for enhancing overall reactor efficiency. Striking a balance between residence time, photon utilization, and mass transfer rates ensures that reactants remain within the reaction zone long enough for effective degradation while avoiding excess catalyst and substrate concentrations that could hinder light penetration. Future advancements in reactor design should focus on combining experimental optimization with CFD simulations to develop scalable, high-performance photoreactors for environmental remediation and sustainable chemical processes.

6. Performance Metrics and Process Evaluation

6.1. Hydrogen Yield and Production Rates

Photoreforming performance is generally quantified by the H_2 evolution rate, often reported in units of micromoles of H_2 per gram of catalyst per hour (μmol H_2 g^{-1} h^{-1}) [125]. Some studies also normalize to the mass of plastic substrate (e.g., μmol H_2 per gram of plastic), especially when focusing on waste conversion efficiency [126]. In general, rates are measured under controlled light conditions (commonly simulated sunlight or UV illumination) and often in alkaline water, which facilitates the breakdown of polymers. Reporting conventions include specifying light intensity (e.g., AM 1.5G, 100 mW cm^{-2}) and reaction time, as many authors report cumulative H_2 yield after a fixed period (e.g., 20 h) in addition to hourly rates. This standardization enables comparison across studies, with values ranging from mere tens of μmol H_2 g^{-1} h^{-1} in early experiments to many mmol H_2 g^{-1} h^{-1} in optimized systems (Table 3).

H_2 production yields via photoreforming vary widely with photocatalyst and plastic type. For example, classic UV-active catalysts, such as TiO_2 loaded with Pt, can achieve high H_2 production rates (on the order of 10^3 μmol g^{-1} h^{-1}) under strong illumination (Table 3). One study reported ~1130 μmol H_2 g^{-1} h^{-1} from PET plastic using Pt/TiO_2 and a 500 W Xe lamp with 5 M NaOH. In contrast, visible-light-driven catalysts such as g-C_3N_4 typically yield lower rates unless modified with co-catalysts [127]. A CN_x|Ni_2P produced in the order of 101-102 μmol g^{-1} h^{-1} of H_2. Uekert et al. demonstrated ambient-temperature photoreforming with CN_x|Ni_2P, achieving roughly

 doi:10.20944/preprints202504.1506.v1

82 μmol H_2 g^{-1} h^{-1} from PET and 178 μmol g^{-1} h^{-1} from PLA under AM 1.5 sunlight [56]. Although less active than noble-metal/TiO_2, metal-free systems are notable for avoiding the use of precious metals.

Doped and composite photocatalysts have shown dramatic improvements in H_2 rates (Table 3). For instance, tailoring semiconductor morphology can enhance performance: mesoporous $ZnIn_2S_4$, a sulfide photocatalyst, delivered ~472 μmol H_2 g^{-1} (from PET, per gram substrate in 20 h) compared to ~178 μmol g^{-1} for conventional ZnIn2S4 under the same conditions [126]. Similarly, a CdS/CdO_x nanocomposite achieved ~132 μmol g^{-1} when utilizing PET as the polymeric entity [57,65]. A $NiCr_2O_4$/TiO_2-$Zn_{0.5}Cd_{0.5}S$ (S-scheme heterojunction) was found to achieve an exceptionally high rate of ~81.4 mmol g^{-1} h^{-1} (81,400 μmol g^{-1} h^{-1}) for H_2 from waste plastics [134], one of the highest reported rates, owing to synergistic light absorption and charge-transfer enhancements. Likewise, ultrathin $NiPS_3$ nanosheets on a CdS photocatalyst enabled solar-driven H_2 evolution of up to ~39.8 mmol g^{-1} h^{-1} for PLA (with ~31.4 mmol g^{-1} h^{-1} from PET) – a rate enhancement of over 1600% compared to bare CdS [128,129]. These examples underscore that catalyst design (bandgap engineering, co-catalyst loading, etc.) greatly influences H_2 output.

Table 3. Hydrogen yield and experimental conditions of each catalyst.

Catalyst	experimental conditions	Hydrogen yield (μmol g^{-1} h^{-1})	Reference
Pt/TiO_2	500 W Xe lamp, 5M NaOH, PET	1130	[125]
CN_x|Ni_2P	AM 1.5 sunlight, ambient temperature, PET	82	[56]
CN_x|Ni_2P	AM 1.5 sunlight, ambient temperature, PLA	178	
Zn|n_2S_4 (mesoporous)	Simulated sunlight, PET	23.6	[130]
Zn|n_2S_4 (conventional)	Simulated sunlight, PET	8.9	
CdS/CdO_x	Simulated sunlight, PET	6.6	[131]
$NiCr_2O_4$/TiO_2-$Zn_{0.5}Cd_{0.5}S$	Visible light, mixed plastics	81.4×10^3	[132]
$NiPS_3$/CdS	Solar-driven, PET	31.4×10^3	[133]
$NiPS_3$/CdS	Solar-driven, PLA	39.8×10^3	
g-C_3N_4/Pt	With NaOH pretreatment, PET	533	[127]
$Au_{0.28}Pd_{0.72}/TiO_2$ HS	5M NaOH, 300 W Xe, PET	0.85×10^3	[125]
MoS_2/CdS	300 W Xe lamp AM 1.5, 10M KOH	PLA: 6.68×10^3 PET: 3.90×10^3 PE: 1.13×10^3	
Co–Ga_2O_3	300 W Xe lamp, AM 1.5, 10M KOH, PE	692	[134]
d-$NiPS_3$/CdS	43× and 1.5× 300 W xenon lamp (PLS-SXE 300), $\lambda > 400$ nm, 2M KOH, PLA	39.76×10^3	[128]

The nature of the plastic substrate has a critical impact on H_2 yields. Generally, plastics containing heteroatoms or functional groups (which are more easily oxidized) yield higher H_2 production than inert polyolefins. Photoreforming polyesters such as PET and PLA tend to be more efficient due to the presence of ester bonds hydrolyzed and oxidized more readily [11,126]. In one study, PLA and PET yielded H_2 in the hundreds of μmol g^{-1} h^{-1} range with a mesoporous sulfide photocatalyst, whereas polyolefins, PP and PE produced only trace amounts of H_2 under identical conditions [126]. The H_2 evolution order was reported as PP < PE < polyacrylate < PET < PLA < polyurethane, correlating with the polymer's susceptibility to oxidative depolymerization. This is due to the systems undergoing pretreatment and depolymerization, which are often prerequisites for robust H_2 generation from resilient polymers. For example, Chang et al. found that alkaline pretreatment (soaking waste PET in NaOH) depolymerized it into monomers, enabling a g-C_3N_4/Pt catalyst to reach a yield of ~533 μmol g^{-1} h^{-1} of H_2 from PET – far higher than yields from untreated plastics like PS or PP (Table 3). Therefore, reported H_2 production rates span a broad range, from less

 doi:10.20944/preprints202504.1506.v1

than 10 μmol g^{-1} h^{-1} for raw polyolefins with unmodified catalysts to ~104-105 μmol g^{-1} h^{-1} for optimized catalysts with easily reformable substrates. It is evident that maximizing H_2 output requires not only advanced photocatalyst materials but also matching them with appropriate feedstock preparation to overcome the recalcitrance of certain plastic wastes.

6.2. Selectivity and Byproduct Formation

In plastic photoreforming, selectivity refers to how the carbon in waste plastics is distributed among various oxidation products. Ideally, one might hope to oxidize the polymer completely to CO_2 (maximizing H_2 yield); however, in practice, the reaction often terminates at intermediate products. As a result, a spectrum of byproducts is formed in the liquid, gas, and solid phases [126]. Understanding these byproducts is crucial because they determine the need for downstream purification and present opportunities for co-product valorization.

6.2.1. Liquid-Phase Organics

A significant portion of the plastic carbon is converted into soluble organic compounds rather than CO_2 [126]. The exact products depend on the polymer structure. For example, the photoreforming of PLA in alkaline water produces lactic acid as a major byproduct, which can further oxidize to pyruvic acid. Studies have illustrated ~61.7 mg of lactic acid and 4.4 mg of pyruvic acid were detected after 12 h from 100 mg of PLA, indicating partial oxidation of the monomer units. Similarly, PET, aromatic polymer, terephthalic acid (TPA), and ethylene glycol (EG) are initially released (via alkaline hydrolysis). During photoreforming, EG was further oxidized to small acids (e.g., acetic acid and 2-hydroxyacetic acid), while TPA largely remained in solution [126]. Other plastics yield analogous fragments: polyurethanes can produce carbamate and alcohol derivatives, and PVC may form chlorinated organics or chloride ions [135–137]. In most cases, no single liquid product dominates; instead, a mixture of short-chain acids (such as formic, acetic, and propionic), alcohols, or oligomers is observed. The formation of these value-added chemicals can be beneficial – for instance, recovered TPA from PET can be repurposed for new polymer production, and organic acids like lactic or formic acid are commercially useful. However, the presence of multi-component organics means the photoreforming solution requires separation steps (e.g., filtration, distillation, or extraction) to isolate H_2 and each byproduct.

6.2.2. Gas-Phase Organics

Besides H_2, oxidized carbon may appear as gaseous byproducts, namely CO_2 or CO (especially under aggressive oxidation conditions). Interestingly, many photocatalytic systems report minimal CO_2 evolution, reflecting high selectivity toward partial oxidation. Studies have reported no CO_2 detectable during PLA/PET reforming with a $ZnIn_2S_4$ catalyst – all carbon was conserved in organic molecules rather than fully mineralized [126]. On the other hand, specific catalysts favor deeper oxidation. A notable product was observed when utilizing a Co-Ga_2O_3 catalyst, which produced a mixture of H_2, CO, and CO_2 from PE, essentially photogasifying the plastic into syngas. The reported H_2, CO, and CO_2 evolution rates were reported as 692.0, 177.8, and 476.4 μmol g^{-1} h^{-1}, respectively [134]. Gas-phase CO (a partial oxidation product) and CO_2 indicate less selective oxidation; however, these greenhouse gases simplify the separation of H_2, as gases can be separated by pressure-swing adsorption or membranes. In a broader context, generating an H_2/CO mixture can be advantageous: syngas can be fed to downstream processes, such as Fischer-Tropsch synthesis or methanol production, effectively valorizing the CO instead of treating it as an undesired emission. However, any CO_2 released represents a loss of carbon efficiency and would need to be captured or offset to maintain environmental benefits.

 doi:10.20944/preprints202504.1506.v1

6.2.3. Solid Residues

Ideally, the plastic should be completely converted in practice; some solid residue can remain, especially for very stable polymers. Incomplete photodegradation of PE or PP, for instance, may result in a waxy or carbonized solid (akin to char or oligomeric fragments that are insoluble) [126]. Photocatalysts that cannot fully break C–C bonds may only surface-oxidize the polymer, resulting in an oxidized polymer residue. In many experiments, pre-grinding or dispersing plastics is used to mitigate mass-transfer limitations, and any residual solids (e.g., unreacted plastic or catalyst fouling deposits) are filtered out after the reaction [138]. Aggressive pretreatments, such as strong bases, plasma, or thermal pre-oxidation, can significantly reduce solid residues by depolymerizing plastics upfront. For instance, a combined plasma-photocatalytic approach was first demonstrated to crack polyolefin chains (via the plasma step) and then photocatalytically reform the volatile products, leaving negligible char [139]. Solid photocatalyst stability is also a consideration, as some catalysts can form deposits, such as coke or polymeric tar, on catalytic surfaces, gradually leading to deactivation. Therefore, maintaining selectivity also involves preventing undesired polymer re-condensation on catalyst surfaces.

6.2.4. Treatment and Opportunities with Byproducts

The presence of byproducts necessitates additional treatment steps; nevertheless, these products also offer opportunities. Gas mixtures containing H_2 will require purification, such as the removal of CO_2 (if present) by scrubbing or separation, especially when fuel-cell-grade H_2 is required. Liquid byproducts in an alkaline solution can be recovered by neutralizing the solution, either by precipitating organic acids or reforming monomers. The recovery of valuable co-products can significantly improve the overall economics. For instance, the organic acids produced can be collected as chemical feedstocks, and monomers such as TPA or glycolate can be recycled back into manufacturing processes. The "photoreforming refinery" concept, which generates H_2 fuel and chemical commodities concurrently, is a key distinguishing feature of plastic photoreforming [36]. High selectivity towards specific useful byproducts is desirable: some studies have aimed for "precision upcycling" of plastics, tuning conditions to produce one dominant organic product (e.g., converting PET mostly to TPA). In summary, unlike water splitting, which yields only H_2 and O_2, plastic photoreforming yields a more complex product slate, requiring integrated separation and purification processes. The challenge and opportunity lie in steering the oxidation toward valuable intermediates while maintaining efficient H_2 extraction.

6.3. Life-Cycle Assessment (LCA) and Techno-Economic Analyses (TEA)

Converting waste plastics to H_2 via sunlight is inherently attractive as a concept. A full life-cycle assessment considers the energy inputs, emissions, and offsets. Photoreforming operates at ambient temperatures and utilizes solar photon energy, resulting in near-zero direct CO_2 emissions during operation [126]. Unlike incineration of plastic (which releases CO_2) or even pyrolysis (which often requires external heating), a solar photoreactor could largely avoid greenhouse gas emissions in the conversion step. Ambient-temperature photoreforming is a low-energy means of transforming plastic waste [55]. No external heat or electricity is required, aside from pumping and, optionally, UV lamps (if natural sunlight is not used). This suggests a potentially favorable carbon footprint: the embedded energy in plastics (initially derived from petrochemicals) is partially recovered as H_2 fuel, and a significant portion of the process energy comes from sunlight. Therefore, LCA must include the energy and emissions associated with catalyst synthesis and the use of any chemicals. For example, if a process requires large amounts of NaOH for pretreatment or other additives, producing and recycling those chemicals incurs an energy cost. Similarly, manufacturing nanoscale photocatalysts, such as through doping and calcination, has an environmental impact. A preliminary analysis indicates that pre-treatment can significantly enhance efficiency, thereby reducing reactor time and size, albeit at the expense of additional chemical input. Consequently, there is an optimal

 doi:10.20944/preprints202504.1506.v1

balance to minimize the overall CO_2 footprint [40,140]. Encouragingly, the feedstock is waste, which means the upstream burden of producing the plastic is allocated to its initial use. In an LCA, the plastic entering a recycling or upcycling process often bears zero or even a negative environmental cost, as it is credited for diverting waste from landfills. By producing H_2 that can displace fossil-derived H_2, photoreforming can offset significant emissions. Findings have shown that H_2 derived from waste could have a significantly lower life-cycle CO_2 footprint than H_2 produced from natural gas, provided that renewable energy drives the process [141]. Additionally, any valuable by-products, such as recovered monomers, offset the need to produce those chemicals from virgin resources, further improving overall sustainability. While detailed LCA studies are still scarce, the consensus is that solar-driven plastic reforming could significantly reduce greenhouse gas emissions compared to conventional disposal and H_2 production routes, as long as the process avoids major non-renewable energy inputs [33].

Early techno-economic analyses suggest that plastic photoreforming, although conceptually green, faces challenges in achieving economic competitiveness. Key cost factors include the catalyst, reactor system, operations, and feedstock preparation (Table 4). The techno-economic feasibility of plastic photoreforming is influenced by several key factors. Catalyst synthesis remains costly, especially when noble metals or complex fabrication steps are involved, though efforts are underway to develop scalable, earth-abundant alternatives with long-term stability [11,56]. Photoreactor design presents another challenge, as systems must efficiently deliver light to catalysts, often requiring large surface areas and transparent materials, which increases capital costs—especially for full-scale applications [142]. While operational costs are relatively low under solar illumination, they rise significantly with the use of artificial lighting or intensive feedstock handling. Feedstock pretreatment, such as alkaline hydrolysis or enzymatic depolymerization, can enhance H_2 yields but adds to the overall cost, with current estimates placing the levelized cost of H_2 (LCOH) at around $50.70/kg, far above conventional methods. Reducing costs through improved catalysts and streamlined pretreatment methods is essential for commercial viability [140].

Table 4. Breakdown of economic factors affecting plastic photoreforming feasibility.

Cost Factor	Key Points
Catalyst Synthesis	- Noble metals improve H_2 yield; however, the materials are costly - Even base-metal systems (Ni, Fe) have synthesis costs - Earth-abundant alternatives (g-C_3N_4 mineral oxides) under study - Catalyst longevity helps spread the cost - Some metal-free systems show multi-day stability
Photoreactor Setup	- Light delivery requires transparent materials, large surface areas - Commercial setups: panels, troughs, floating systems - High capital cost due to quartz/glass, mirrors, CPCs - The modular scale-up appears feasible (2 mL → 120 mL) - Full-scale systems need thousands of liters, adding complexity
Operational Costs	- Low cost under sunlight, minimal energy input - Operational needs: pumping, stirring, catalyst replacement - Artificial light (UV/LED) increases cost dramatically - Conventional steps (shredding, washing) are low cost - Advanced pretreatments (plasma, enzymes) raise OPEX
Feedstock Pretreatment	- NaOH/KOH hydrolysis is common but adds chemical cost - Base recovery adds complexity - Enzymatic routes are mild but expensive - LCOH ~ $50.70/kg H_2 (base pretreatment) - Cost reduction is possible via cheaper methods or active catalysts

 doi:10.20944/preprints202504.1506.v1

Considering these factors, current TEA studies suggest that plastic photoreforming is not yet cost-competitive with conventional H_2 production. For instance, H_2 produced from large-scale natural gas reforming costs around $1.50 per kg, and even electrolysis with renewable power aims for less than $5 per kg. In comparison, the first estimates for photoreforming are one to two orders of magnitude higher in cost [140]. However, these analyses also highlight levers for cost reduction. If the feedstock is considered free (or has a negative cost, as municipalities may pay for waste processing), and if co-product revenues are accounted for by selling organic byproducts, the economics improve. Studies have shown that generating salable chemicals (such as diesel-range hydrocarbons or monomers) alongside H_2 could offset enough costs to roughly halve the levelized cost of H_2 production of the process [143]. Another important factor is scale: many renewable technologies start out as expensive but decrease in cost with scale and technology advancement. Photoreforming may leverage advancements in photocatalytic water splitting and solar reactor design being developed within the energy research community. Moreover, integrating photoreforming with existing waste management infrastructure could help defray costs (for example, by siting photoreactors at landfills or wastewater treatment plants that already collect waste and have available land area). In LCA/TEA terms, the "credit" for avoiding plastic pollution and the environmental benefit of preventing landfill or incinerator use is significant but not easily monetized. Some analyses suggest that if carbon credits or pollution penalties are factored in, photoreforming's value proposition becomes stronger, despite higher upfront costs [9]. Even though current economics are challenging, there are clear pathways (such as cheaper catalysts, co-product valorization, and policy incentives) that could move plastic photoreforming toward viability in the future.

6.4. Comparative Benchmarking

Benchmarking against other H_2 production methods highlights the unique niche of plastic photoreforming as well as the hurdles it must overcome for commercial deployment. Traditional photocatalytic water splitting utilizes sunlight to split pure water into H_2 and O_2. The oxygen evolution half-reaction is highly endothermic and kinetically slow, which limits the overall efficiency. Water splitting also doesn't depend on a supply of waste – it can run anywhere with water and sunlight, whereas plastic photoreforming targets a very specific feedstock. In terms of maturity, photocatalytic water splitting has been studied for decades; plastic photoreforming is a relatively new approach that can leverage some of the same advances, such as the development of new photocatalyst materials. A critical factor for photoreforming is that it must not only generate H_2 efficiently but also handle the carbon in a way that adds value or at least causes no harm. Water splitting doesn't have this burden. Thus, if the goal is purely to produce renewable H_2, water splitting sets the benchmark (with no carbon involved); however, photoreforming makes sense as a complementary route that also addresses the elimination of waste plastic. A future sustainable energy system could utilize water splitting for H_2 when sunlight and clean water are abundant and switch to photoreforming in contexts where organic waste is available as a feedstock, thereby producing H_2 while recycling the waste.

Photocatalytic reforming is not limited to plastics – numerous studies have utilized biomass-derived substrates, including sugars, glycerol, and cellulose, to produce H_2. In fact, biomass photoreforming is generally easier than plastic because biomolecules are more labile [14]. For example, methanol photoreforming proceeds readily at much lower light energies than water splitting, and lignocellulosic waste can be broken down by photocatalysts into H_2 and CO_2 or small organics with fewer barriers, as biomass often contains oxygen and functional groups that facilitate degradation [144]. Plastics are more inert than these, especially polyolefins, which are essentially long hydrocarbon chains with no polar groups. As a result, benchmark H_2 rates for biomass reforming are often higher. Indeed, reported H_2 yields from photocatalytic lignocellulose reforming or even microalgae can reach several mmol g^{-1} h^{-1} under similar light conditions, outpacing many early plastic reforming results [125].

 doi:10.20944/preprints202504.1506.v1

However, plastic photoreforming targets a problematic waste stream that biomass methods do not address – waste plastics are increasing in volume and do not decompose biologically. In contrast, biomass is renewable and already part of the natural carbon cycle. In terms of outputs, biomass reforming usually fully mineralizes the substrate to CO_2 (especially if the goal is maximal H_2), whereas plastic photoreforming, as noted, tends to stop at intermediates. Some recent research blurs the line between biomass and plastics, for instance, co-photoreforming mixtures of plastic and biomass or using bio-derived enzymes to preprocess plastics [140]. Such hybrid approaches aim to harness the easier degradability of biomass to kickstart plastic breakdown. In summary, biomass photoreforming sets an upper benchmark for performance, as those substrates are easier to reform. Plastic photoreforming is gaining momentum by employing similar catalytic strategies, such as adapting catalysts developed for glycerol to work with polymers. However, it must overcome the greater stability of plastic polymers. Notably, both processes share some scalability issues, such as handling solid feeds and mass transfer, and both offer the appealing concept of a "solar refinery" – utilizing sunlight to produce H_2 fuel and value-added chemicals from waste.

The ultimate yardstick for H_2 generation is industrial technologies, such as steam methane reforming (SMR), coal gasification, and, increasingly, water electrolysis [141]. SMR (from natural gas) produces the bulk of the world's H_2 at a cost of $1–2 per kilogram of H_2; however, the system emits ~9 kilograms of CO_2 per kilogram of H_2 and relies on fossil fuels. Coal gasification has even higher emissions. Plastic photoreforming, if successful, could offset some of the fossil H_2 by providing a green H_2 source and consuming waste plastic, thereby addressing two environmental issues simultaneously [56]. However, in terms of efficiency and throughput, photoreforming is currently far behind SMR – sunlight is a diffuse energy source, and photocatalytic rates (even in the best cases, which are typically in the tens of mmol g^{-1} h^{-1}) are many orders of magnitude lower than the thermal reaction rates in an SMR plant. Additionally, SMR produces H_2 continuously from a constant gas stream, whereas photoreforming would likely be a batch or semi-batch process dealing with slurries of solid waste. Photoreforming's advantage is its virtually zero feedstock cost and carbon-neutral (or even carbon-negative) footprint, which SMR cannot match. Compared to electrolysis, photoreforming doesn't require an external electrical input – the solar energy is harvested directly by the catalyst. Water electrolysis coupled to solar PV is a competing sustainable route to H_2. Photoreforming might have an edge when feedstock cost is considered: electrolysis requires pure water (which has a cost and can be scarce) and yields only H_2 (with no co-products), whereas photoreforming "pays for itself" partly by treating waste. That said, electrolysis technology is far more mature; large electrolysis plants (greater than 100 MW) are being built now, whereas photoreforming is still at the lab prototype stage. A techno-economic analysis noted that H_2 from waste, via pyrolysis or gasification, could potentially reach costs in the $1.4–4.8 per kg range, comparable to electrolysis, if scaled efficiently (Figure 7) [141]. This suggests that if photoreforming can significantly improve its efficiency (perhaps via better light utilization, photocatalyst quantum yields, and continuous flow designs), it could eventually compete on cost, especially since it sidesteps the electricity-to-hydrogen conversion losses inherent in electrolysis.

 doi:10.20944/preprints202504.1506.v1

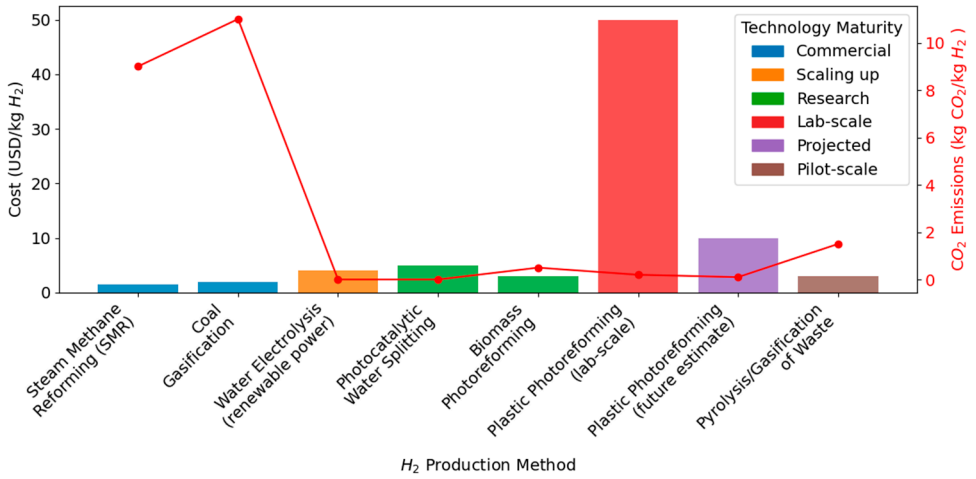

Figure 7. Comparison of H_2 production methods: cost vs. CO_2 emissions.

Regardless of the comparison, several critical factors will determine whether plastic photoreforming can transition from a lab curiosity to an industrial application. Among these parameters, the solar-to-hydrogen (STH) efficiency must increase. Current STH efficiencies are often well below 10%. To be practical, much higher efficiencies (15% - 25%+) are needed so that reasonable reactor areas can generate significant H_2. This ties to improving catalyst light absorption (e.g., extending the response into the visible spectrum), minimizing charge-carrier recombination, and ensuring that each photon absorbed leads to a useful chemical reaction [11]. The impressive rates achieved with novel catalysts (e.g., $NiPS_3$/CdS or $NiCr_2O_4$/TiO_2-CZS) are encouraging; nevertheless, these must be reproducible in larger, real-sunlight systems [125,145]. Efficiently illuminating a reactor full of plastic and catalyst is non-trivial. Light attenuation, mixing, and mass transport limit the reactor depth. Scale-up may require thin, sheet-like reactors or transparent devices through which slurry flows. Alternatively, immobilizing the photocatalyst on surfaces (to avoid filtration) while still allowing it to contact the plastic presents an engineering challenge. Full-scale also implies moving from idealized pure plastics to mixed waste streams. A commercial system would need to handle a heterogeneous mix of plastics, possibly contaminated with food or other debris [56]. Robust pretreatment (such as shredding, washing, and possibly chemical dosing) will be required, adding complexity; however, it will align with the existing skill set of waste management operations.

For long-term operation, photocatalysts must resist deactivation and maintain their durability. Fouling by byproducts, photochemical corrosion (e.g., CdS can photocorrode to Cd^{2+} in solution), or loss of co-catalysts (like metal nanoparticles sintering or detaching) are concerns [56]. Frequent replacement of catalysts would drive up costs, so research focuses on stable materials (e.g., TiO_2 is very stable under UV, carbon nitrides are fairly stable under visible light, etc.). Encapsulation of photosensitive, however, active catalysts or the development of self-cleaning surfaces (to shed coke and deposits) could improve longevity. In an industrial benchmark, catalysts should ideally last months or possibly years, with minimal activity loss, which is a tall order given most lab tests run days at most. The photoreforming process must be integrated with separation units for H_2 and for any liquid products. If the goal is pure H_2, one might integrate a membrane that allows H_2 to escape continuously from the reactor [56]. This would prevent the buildup of pressure and remove H_2 to avoid reverse reactions. Liquid products could be periodically drained and processed (e.g., distilled to separate organics from the aqueous alkali). The need for these additional units means that a photoreforming plant begins to resemble a chemical plant with multiple sections, including reaction, separation, and recycling of unreacted materials. Designing this in a simple, possibly modular way will impact viability. One concept is a modular photoreforming unit that can be deployed at remote locations, much like a solar-powered "waste-to-hydrogen" unit on site. This has appeal for, say, off-grid communities or island nations where plastic waste is plentiful and H_2 could be used for energy.

 doi:10.20944/preprints202504.1506.v1

Finally, when benchmarking photoreforming, one must consider that mechanical recycling and other forms of chemical recycling, such as pyrolysis and hydrolysis, are also competing to handle waste plastics. Photoreforming will be most attractive for plastics that are not easily recycled by other means, such as dirty, mixed, or non-polyester plastics, where mechanical recycling yields low-quality output [56]. It may also find use in destroying microplastics or plastic pollutants in water, where the simultaneous generation of H_2 adds value to environmental cleanup. If mechanical recycling can be done, it is usually more energy-efficient to melt and remold plastic than to break it into H_2. Therefore, photoreforming's niche is likely non-recyclable plastic waste, which is indeed the focus of several studies. In that niche, its competition is landfill or incineration – and against those, photoreforming fares very well on an environmental basis, with no toxic emissions and useful outputs. The technology that perhaps comes closest is the gasification/plasma conversion of waste to syngas, which is commercially piloted. Gasification operates at high temperatures but is less selective, producing CO_2 and CO and requiring an energy input. Photoreforming is the low-temperature, solar-driven counterpart, trading speed for selectivity and sustainability.

In conclusion, plastic photoreforming is a promising and multifaceted approach at the intersection of renewable energy and recycling. When benchmarked against other H_2 production methods, it stands out by addressing two problems simultaneously: clean energy and plastic waste. Its current performance is below that of mature technologies; however, rapid advances in catalyst efficiency and a deeper understanding of reaction pathways are closing the gap. The ultimate viability will depend on achieving competitive H_2 production rates and demonstrating that the process can be scaled and integrated in a cost-effective and sustainable manner. Each comparison — with water splitting, biomass reforming, and conventional H_2 production — provides both inspiration and perspective: photoreforming doesn't need to replace those methods outright; however, if it can complement them by utilizing waste as a resource, it could carve out a valuable role in the future H_2 economy. The next decade of research and pilot demonstrations, guided by TEA/LCA insights, will determine whether solar-driven upcycling of plastic to H_2 can transition from lab curiosity to a commercially deployed reality.

7. Environmental and Sustainability Perspectives

7.1. Waste Management and the Circular Economy Context

Photocatalytic plastic photoreforming provides a means to convert difficult-to-recycle plastics into valuable products, such as H_2 fuel, thereby complementing conventional recycling methods. Currently, only about 9% of plastic waste is recycled, and nearly 79% ends up in landfills or the natural environment [146]. By targeting non-recyclable plastics (e.g., contaminated, or mixed waste), photoreforming could divert a significant fraction of this waste from landfills. Recent demonstrations show that real-world plastic waste (such as polyester microfibers or oil-contaminated PET) can be photoreformed into H_2 and organic chemicals [56]. This indicates that photoreforming can be integrated as an upcycling step in recycling facilities, simultaneously eliminating plastic waste and generating useful fuels. Such integration would reduce pollution and landfill volumes while providing an economic incentive (in the form of H_2 yield) to reclaim plastics rather than discard them.

7.2. Waste Management and the Circular Economy Context

During photocatalytic plastic degradation, the polymer can break large polymer chains into smaller fragments; however, if the process is incomplete, it may generate microplastics or nanoplastics as interim fragments (Figure 8) [147]. The absence of conversion to CO_2 means that polymers pass through various oxidized organic intermediates. Partial oxidation of polymers yields a spectrum of smaller compounds such as alcohols, aldehydes, ketones, carboxylic acids, and hydroxy acids [148]. For instance, polyolefins such as PE and PP tend to form long-chain oxygenated products, including long-chain alcohols and acids, in their soluble oxidized fractions. Aromatic polymers behave differently; PS photodegradation produces aromatic intermediates, with benzoic

 doi:10.20944/preprints202504.1506.v1

acid and terephthalic acid (1,4-benzenedicarboxylic acid) identified as major byproducts. These intermediates have been confirmed via spectroscopic and chromatographic analyses [149,150]. Eventually, the continued photocatalytic attack can break down these intermediates to CO_2 is observed as the main final product once oxidation runs to completion [147]. The presence of carbonyl (C=O) and hydroxyl (–OH) functional groups on partially oxidized plastics, as observed from FTIR, validates these intermediate byproducts. Identifying and characterizing such intermediates is crucial, as it informs whether the process stops at potentially harmful chemicals or proceeds to full mineralization.

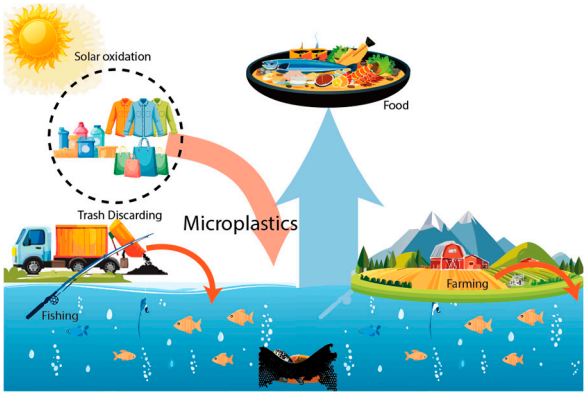

Figure 8. General representation of discharge and transportation of microplastics in the ecosystem.

In the situations of photocatalytic treatment is incomplete, the release of microplastics and oxidative byproducts poses environmental risks. Micro- and nanoplastics are persistent pollutants that can accumulate in aquatic and terrestrial environments, where they present physical and chemical hazards to organisms [147]. These small plastic particles can be ingested by wildlife, potentially causing digestive blockages, reduced feeding, and the transfer of pollutants up the food chain. Moreover, microplastics can act as vectors for other contaminants – they sorb and carry persistent organic pollutants and heavy metals on their surfaces, compounding ecological risks [147]. The chemical additives in plastics, such as stabilizers, plasticizers, and flame retardants, also leach out during degradation. As plastics fragment and age, additives not chemically bound in the polymer matrix can dissolve into water, posing ecotoxicological risks [151]. Many of these additives (and their degradation products) have toxic or endocrine-disrupting effects, yet their identities and impacts are not fully understood.

As a result, there is growing concern regarding the formation of partially oxidized byproducts during the photoreforming process. These intermediate compounds (e.g., short-chain acids, aldehydes, phenolics) may be more bioavailable and toxic than the original polymer. For example, laboratory aging of plastics has shown that oxidized oligomers can leach out and potentially affect microorganisms and animals [148]. Biale et al. emphasize that pollution by microplastics is not just about the solid particles but also "the small, oxidized species that may leach out" of those particles, which could have their own toxicity. Therefore, an important part of risk assessment is evaluating the toxicity and fate of intermediate byproducts in addition to the physical microplastics [152]. Environmental studies and LCA are increasingly calling for photocatalytic systems that either trap and fully degrade these byproducts or ensure they are harmless before any release [153].

To prevent the formation of persistent microplastics or toxic byproducts, current studies are developing strategies to drive photocatalytic reactions to complete mineralization. This includes enhanced oxidation conditions, utilizing additives or operational tweaks to generate more reactive species and prevent the early termination of the reaction. For example, adding electron acceptors (such as persulfate) can suppress charge-carrier recombination and boost $^{\bullet}OH$ radical production, leading to more complete oxidation of plastic residues [154]. Optimized catalysts under UV light have achieved a conversion of over 98% of microplastic carbon to CO_2 in hours, demonstrating that aggressive oxidation conditions can eliminate nearly all organic remnants. Pre-treatment and

 doi:10.20944/preprints202504.1506.v1

fragmentation facilitate the breakdown of bulk plastics into smaller sizes before or during photocatalysis, thereby enhancing surface area and catalyst contact [54,154,155]. Optimized catalysts under UV light have achieved a conversion of over 98% of microplastic carbon to CO_2 in hours, demonstrating that aggressive oxidation conditions can eliminate nearly all organic remnants. Pre-treatment and fragmentation facilitate the breakdown of bulk plastics into smaller sizes before or during photocatalysis, thereby enhancing surface area and catalyst contact [54,155]. Mechanical milling of plastic waste into micro-scale particles has been shown to accelerate subsequent photocatalytic degradation [156]. Smaller fragments (or thinner fibers) allow more efficient light penetration and oxidant access, ensuring that no large unoxidized core remains. Similarly, swelling or softening plastic (via solvents or thermal pretreatment) can increase the polymer's susceptibility to photochemical attack. Multistep and combined processes are often necessary to degrade stubborn intermediate oligomers that resist direct photocatalytic conversion effectively [157]. A recent study on PET photoreforming introduced a mild chemical activation step (using H_2PdCl_4) that breaks insoluble high-molecular-weight fragments into simpler compounds, which are then more easily mineralized under light [158]. Such approaches target the typically recalcitrant byproducts, such as waxy or char-like residues, that pure photocatalysis may leave behind. In other cases, combining photocatalysis with Fenton or photo-Fenton reagents ($^{\bullet}OH$ from Fe/H_2O_2) has been successful in degrading microplastics that resist direct photolysis [159]. However, the overarching strategy is to leave no persistent pollutant: any intermediate that isn't mineralized by one method is subjected to another until complete degradation is achieved [156]. Achieving complete photoreforming of plastics without generating microplastic byproducts heavily relies on innovations in photocatalyst design and reactor engineering. High-activity photocatalysts, such as traditional TiO_2 photocatalysts, are effective under UV but can be limited by fast charge recombination and a lack of visible-light absorption [10]. Recent studies focus on doping and composite strategies to enhance performance, namely, the introduction of carbon and nitrogen that creates mid-gap states, extending its activity into visible light and improving microplastic degradation rates [160]. Similarly, coupling TiO_2 or ZnO with co-catalysts (e.g., depositing noble metals or coupling with other semiconductors) boosts efficiency (Section 4.3). Plasmonic Pt-ZnO nanorods have demonstrated enhanced visible-light degradation of microplastic fragments compared to bare oxides [161]. Recent studies focus on doping and composite strategies to enhance performance, namely, the introduction of carbon and nitrogen that creates mid-gap states, extending its activity into visible light and improving microplastic degradation rates [160]. Similarly, coupling TiO_2 or ZnO with co-catalysts (e.g., depositing noble metals or coupling with other semiconductors) boosts efficiency (Section 4.3). Plasmonic Pt-ZnO nanorods have demonstrated enhanced visible-light degradation of microplastic fragments compared to bare oxides [161]. Such composites harness a broader solar spectrum and generate more radicals, thereby reducing the chance of partially oxidized leftovers. Novel photocatalysts beyond the usual oxides – e.g., bismuth oxyhalides (BiOCl) and Cu_xO semiconductors – have shown activity against microplastics. In the near future, metal-free photocatalysts like graphitic carbon nitride ($g\text{-}C_3N_4$) are expected to play a role, given their success in removing other organic pollutants (Section 4.2). These new materials aim to maximize quantum efficiency and generate powerful oxidizing species so that plastics are fully broken rather than merely shattering into micro-debris. Reactor and contact engineering play a crucial role beyond the catalyst itself, as the reactor configuration is essential in mitigating microplastic formation. One advance is the use of immobilized catalysts in structured reactors that improve contact with plastic pollutants. For instance, TiO_2-coated β-SiC foam monoliths have been employed in flow-through reactors to treat plastic suspensions, achieving substantial total organic carbon removal (~50% in 7 hours for polymethyl methacrylate microplastics) while allowing for continuous operation [162]. Such designs prevent the escape of partially degraded particles by keeping them in a reactive environment until complete breakdown occurs. Another innovative concept is the development of self-propelled photocatalytic micromotors. Chattopadhyay et al. created TiO_2 "Pac-Man" micromotors that actively swim in water, latch onto microplastic particles, and degrade them in situ [163]. These microscale robots use photocatalytic propulsion to

 doi:10.20944/preprints202504.1506.v1

corral microplastics, ensuring close contact for efficient oxidation. By combining physical collection with chemical degradation, they significantly reduce the likelihood that any microplastics escape treatment. Additionally, researchers are integrating photocatalysts into membrane filters and coatings, allowing water to pass through while simultaneously capturing and oxidizing plastics. Examples include N-doped TiO_2 coatings on filter surfaces that achieved a measurable breakdown of microplastic particles during filtration [164]. All these reactor innovations share the common goal of maximizing interaction between plastics and photoactive surfaces so that even tiny fragments are continuously exposed to oxidative radicals until they are completely mineralized. This holistic design approach minimizes the formation and release of microplastics in photocatalytic systems.

7.3. Policy and Regulatory Landscape

Supportive policies play a pivotal role in accelerating the adoption of plastic photoreforming by recognizing its environmental and economic benefits. Many governments are incentivizing green H_2 production, including H_2 derived from renewable or waste-based sources. For instance, the United States has introduced tax credits of up to $3 per kilogram for clean H_2 production [165,166]. Such financial incentives improve the viability of H_2 sourced from waste plastics, potentially making photoreforming more competitive with conventional fossil-fuel-derived H_2. Extended Producer Responsibility (EPR) policies are increasingly being implemented to shift the burden of plastic waste management onto producers. These policies mandate that producers contribute to the costs associated with plastic waste collection, recycling, and disposal. In Europe, EPR initiatives have led to increased plastic waste recovery, with Germany and the UK demonstrating successful implementations of these frameworks [165]. For example, Germany has adopted a dual-system approach, where companies are required to take back used packaging and contribute to recycling initiatives, thus ensuring a steady supply of waste plastics that could be redirected toward photoreforming.

While existing policies are making strides toward reducing plastic pollution, additional legislative support is necessary to scale up advanced recycling technologies such as photoreforming. Future regulatory measures could focus on:

- **Increased R&D Funding:** Governments could allocate research grants to accelerate the development of high efficiency photocatalysts and scalable reactor designs.
- **Market-Based Incentives:** Carbon credits or renewable energy credits could be extended to photoreforming projects.
- **Mandated Recycled Content:** Setting minimum thresholds for recycled plastic usage in industrial applications could further drive investment in advanced recycling technologies.

Overall, strong policy support, including H_2 incentives, EPR enforcement, and waste reduction mandates, creates a favorable environment for integrating plastic photoreforming into the broader waste management and energy sectors.

8. Challenges and Future Directions

8.1. Technical Hurdles

Plastic photoreforming is often limited by low quantum yields and slow H_2 evolution rates [167,168]. One of the challenges is that many photocatalysts only harvest UV light (~4% of sunlight), leaving most of the solar spectrum unused. Moreover, rapid charge-carrier recombination competes with the redox reactions; photogenerated electrons and holes can recombine in nanoseconds, whereas surface oxidation of plastics is much slower (milliseconds to seconds). These kinetic mismatches severely curb efficiency. Strategies to improve rates focus on materials engineering to broaden light absorption and suppress recombination. For example, creating oxygen vacancies in TiO_2 by high-pressure phase alteration has been shown to enhance visible-light absorption and prolong charge

 doi:10.20944/preprints202504.1506.v1

separation, boosting H_2 output during PET photoreforming [15]. Similarly, tailoring g-C_3N_4 structure can dramatically improve activity – melamine-derived g-C_3N_4 with Pt co-catalyst achieved ~7.3 mmol H_2 $g^{-1}{\cdot}h^{-1}$, far outperforming other variants, thanks to its higher crystallinity, reducing defect recombination [169]. Such advances demonstrate that rational catalyst design, including defect engineering and optimized crystal phases, can enhance photoreforming rates closer to practical requirements.

Photocatalyst durability is also a critical factor for any sustained H_2 production process. In practice, many catalysts suffer from gradual deactivation due to photo-corrosion, fouling, or structural breakdown [168]. For instance, sulfide photocatalysts (e.g., CdS) can photocorrode or leach toxic ions, losing activity [56]. Real plastic wastes can also release additives (dyes, halogens, etc.) that poison active sites by forming inhibiting byproducts on the catalyst surface. Over time, photocatalyst crystals may lose crystallinity, and active sites become occluded by reaction intermediates or polymer residues, causing performance to drop. Robust catalyst design and operating strategies are needed to combat these effects. Developing cocatalysts that resist poisoning (e.g., Ni_2P instead of noble metals) and using protective layers or supports can improve longevity. Notably, carbon nitride/nickel phosphide systems have demonstrated stable H_2 production over days of operation – one study showed a CN_x|Ni_2P catalyst remained active for >18 days until all plastic substrate was consumed. Its stability is attributed to strong catalyst–substrate interactions and an avoidance of self-degradation pathways. In contrast, simply boosting initial activity (e.g., by N-doping CN_x) can trade off stability – doping increased H_2 yield but led to faster deactivation in long runs. Therefore, a balanced approach is required: catalysts must not only be active but also resist deactivation mechanisms like photooxidation, leaching, or surface fouling. Research is actively exploring durable photocatalysts (e.g., oxynitrides, phase-stable composites) and regeneration methods to ensure long-term performance [11].

Real-world plastic waste is heterogeneous and often contaminated, posing a major hurdle for photoreforming. Impure feeds can introduce light attenuation and inhibitors. Colored plastics or additives absorb/scatter light, effectively "stealing" photons that the catalyst needs [167]. Turbid slurries of mixed waste limit light penetration, especially in scaled reactors. Additionally, common additives (e.g., stabilizers, fillers, chlorine from PVC) can scavenge reactive radicals or poison catalysts, severely reducing H_2 yields. To address this complexity, pretreatment and adaptive reactor strategies are employed. For example, one approach is chemical/enzymatic pretreatment to depolymerize plastics into smaller, soluble compounds that are more amenable to photocatalysis. Recent studies demonstrated that soaking resilient polymers like PP, PS, or PVC in 40-70°C NaOH for hours can break them into monomers, which are then readily photoreformed to H_2 [64,170]. This tandem depolymerization-photoreforming strategy significantly improved the conversion of "inert" plastics. Similarly, combined processes (chemo-enzymatic routes) have been proposed, where enzymes first digest the polymer into oligomers that the photocatalyst can oxidize efficiently [140,171]. Even without extensive pretreatment, some advanced catalysts can tolerate mixed wastes: a CN_x|Ni_2P photocatalyst was shown to generate H_2 from real municipal waste samples, including microplastic fibers and food-contaminated plastics, when run in alkaline water [56]. However, careful reactor design, including agitation and illumination geometry, was necessary to maintain efficiency at a larger volume. Overall, handling waste stream complexity requires (i) removing or mitigating inhibitors (through sorting or pretreatment to eliminate toxic elements and soluble impurities) and (ii) designing catalysts and reactors that can operate with impure, opaque feeds. Developing photocatalysts that are poison-resistant and active in complex media is an active area of research, crucial for translating lab-scale photoreforming to practical applications for waste plastics.

8.2. Materials Innovation

Achieving breakthrough performance in plastic photoreforming will likely require novel photocatalyst materials beyond the traditional TiO_2 and g-C_3N_4. Researchers are exploring materials that offer wider light absorption, higher activity, and greater durability. Perovskite-based systems

 doi:10.20944/preprints202504.1506.v1

are one promising avenue; for example, bias-free photoelectrochemical cells using halide perovskite photoabsorbers have been designed to simultaneously oxidize soluble plastic waste on one electrode while generating H_2 on the other [172]. These tandem devices leverage the excellent visible-light absorption of perovskite semiconductors, though stability (especially in aqueous conditions) remains a challenge. Another cutting-edge approach is the use of high-entropy oxides/oxynitrides as photocatalysts. By incorporating five or more different cations into a single lattice, high-entropy materials can exhibit synergistic electronic effects and defect chemistry not found in conventional catalysts. A recent study introduced a high-entropy oxynitride (Ti-Zr-Hf-Nb-Ta-N) for PET photoreforming, which achieved superior H_2 and organic product generation compared to the parent oxide [11]. The nitrogen incorporation distorted the lattice and narrowed the bandgap, dramatically enhancing visible-light activity and charge separation. Such materials also showed excellent stability under illumination, addressing longevity concerns. Single-atom catalysts (SACs) are another visionary solution: isolating metal atoms (e.g., Pt, Ni, Co) on a support can maximize active site exposure and tunability. To date, SACs have rarely been applied to plastic photoreforming, but experts see big potential [168]. For instance, single-Pt-atom decorated carbon nitride has been proposed to efficiently drive H_2 evolution with minimal precious metal loading. Similarly, dual-atom and cluster catalysts could provide cooperative active sites for simultaneous plastic oxidation and H_2 evolution [173–175]. Currently, SACs have rarely been applied to plastic photoreforming, but experts see big potential [168]. Tandem systems are also envisioned, where two (or more) coupled photocatalysts target different steps: one optimized for polymer oxidation and another for H_2 evolution, working in concert (e.g., Z-scheme heterojunctions linking a strong oxidizer with a H_2-generating semiconductor) [168]. Lastly, catalyst recyclability and reusability are being factored into the design [176]. Future photocatalysts may be engineered on insoluble supports or as easily recoverable frameworks, such as photocatalytic metal-organic frameworks or robust polymer films, to allow for repeated use without performance loss [177,178]. Lastly, the recyclability and reusability of catalysts are being factored into the design. The ultimate vision is a new generation of photocatalysts that are highly active under sunlight, robust against deactivation, and constructed from earth-abundant elements – this could include advanced doped semiconductors, 2D materials (such as MXenes and graphitic carbon nitride derivatives), and plasmonic composites that utilize the full solar spectrum.

To fully harness sunlight for H_2 production from waste, photocatalysts must be tailored for strong visible-light absorption and efficient utilization of charge carriers. This involves bandgap engineering and nanostructuring to optimize how a material absorbs photons and transports electrons and holes. Translating plastic photoreforming from benchtop reactors to the industrial scale presents significant engineering challenges. Conventional slurry reactors, where powdered photocatalyst is dispersed in a plastic waste solution, encounter problems when scaled up: ensuring uniform light distribution, preventing catalyst agglomeration, and handling opaque mixtures are non-trivial. As reactor volumes increase, photocatalyst particles tend to settle or clump, leading to inefficient illumination and reaction "dead zones." Continuous flow operation will be crucial for commercialization, replacing batch setups with systems that can steadily process incoming waste. Early demonstrations of continuous photoreforming (as in the panel reactor) are encouraging, although further work is needed on reactor throughput, fouling management (e.g., removing solid residues), and integration with pre- and post-processing units (for feed preparation and product recovery). Ultimately, scalable photoreforming may be implemented in specialized solar reactors at recycling centers or landfills, where sunlight can be harnessed to treat waste streams on-site. Reactor engineering innovations –from catalyst immobilization and modular reactor scaling to light management– are paving the way toward larger-scale, real-world photoreforming applications.

For plastic photoreforming to be commercially viable, it must produce H_2 at costs competitive with conventional methods like SMR or water electrolysis. Encouragingly, preliminary techno-economic analyses suggest photoreforming could achieve favorable economics under optimized conditions. The range of current fossil-derived "grey" H_2 ($1–2 per kg) and lower than most "green"

 doi:10.20944/preprints202504.1506.v1

H_2 from electrolysis (often $4–6 per kg) [179,180]. Several factors give photoreforming a potential economic edge: it utilizes solar energy, which is free, and plastic waste feedstock, which is either cheap or even has a negative cost (municipalities may even pay to dispose of it). In essence, photoreforming piggybacks on waste management – it can be seen as waste treatment that generates fuel. This dual benefit means the process could earn credits for waste reduction while producing H_2. Moreover, the mild reaction conditions (ambient temperature and pressure) translate to lower equipment and operational costs compared to high-temperature SMR (steam methane reforming) or gasification [56]. However, there are important caveats and current weaknesses. Photoreforming is an inherently intermittent technology (dependent on sunlight); thereby, consistent H_2 output would require energy storage or hybrid systems to buffer night-time or cloudy-day production. The land area required for solar capture can be substantial for significant H_2 volumes, which may limit deployment in densely populated areas. Additionally, while the feedstock is "free" in principle, collecting, sorting, and preprocessing waste plastics entail logistical costs that must be factored into the equation.

In summary, photoreforming uniquely merges waste remediation with fuel production, operating at ambient conditions with only sunlight as the energy input [56]. Its major strengths are sustainability (converting an environmental liability into clean H_2) and potentially low operating cost since neither high-pressure reactors nor external fuel/energy are required (Figure 9) [12]. It produces H_2 without direct CO_2 emissions and can generate valuable co-products from plastic carbon, unlike water electrolysis, which only yields oxygen as a byproduct. Compared to SMR, photoreforming avoids fossil feedstock and greenhouse gases; however, it currently lags in reaction rate and scale. SMR can continuously produce large H_2 volumes but at the cost of CO_2 emissions and energy-intensive operation. Compared to electrolysis, photoreforming doesn't require expensive electricity or pure water and can achieve the difficult water oxidation step more easily by using plastics as sacrificial donors (bypassing the slow oxygen evolution reaction) [12]. However, today's electrolysis technologies have higher technological readiness and can reach higher solar-to-hydrogen efficiencies when coupled with photovoltaic power, whereas photoreforming is still improving its quantum efficiencies. In short, the weaknesses of plastic photoreforming are its early-stage development, relatively low H_2 output per reactor volume, and dependence on sunlight, as well as the variability introduced by real-world waste [181]. Its strengths lie in sustainability and integrative value: it addresses two problems (plastic waste and clean fuel) simultaneously, which could justify its adoption even if pure economic metrics are marginal. With continued innovation in catalysts, reactors, and systems integration, the gap between photoreforming and incumbent H_2 technologies is expected to narrow, positioning photoreforming as a key player in a future circular H_2 economy [66].

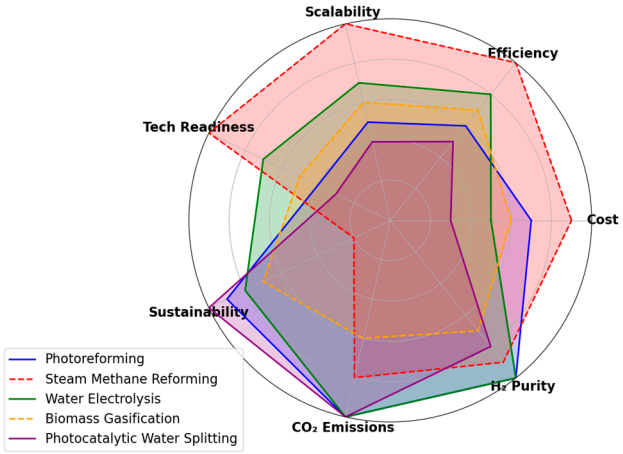

Figure 9. Techno-economic and environmental comparison of H_2 production technologies.

 doi:10.20944/preprints202504.1506.v1

9. Conclusions

Plastic photoreforming represents a transformative approach at the intersection of waste valorization and clean energy generation. By harnessing solar energy to convert non-recyclable plastics into H_2 fuel and valuable chemical intermediates, this process offers a sustainable pathway to address the dual global crises of plastic pollution and greenhouse gas emissions. The reviewed advances in photocatalyst engineering—ranging from bandgap-tuned semiconductors and heterojunction composites to metal-organic frameworks and single-atom catalysts—have significantly improved H_2 production rates, light absorption, and charge-carrier dynamics. Similarly, innovations in reactor design, pre-treatment strategies, and light management are pushing the boundaries of photoreforming performance and scalability.

Despite these encouraging developments, several critical challenges remain. Achieving commercially viable H_2 production hinges on overcoming low quantum efficiencies, improving catalyst durability under real-world conditions, and developing systems capable of handling heterogeneous and contaminated plastic waste streams. The formation of microplastic residues and toxic byproducts during partial degradation also necessitates the development of integrated treatment systems and robust risk mitigation strategies to ensure environmental safety. Techno-economic analyses reveal that while photoreforming is not yet cost-competitive with incumbent H_2 production methods, such as steam methane reforming or water electrolysis, its potential for low-cost operation, driven by free solar energy and negative-cost feedstock, offers a unique value proposition. Life-cycle assessments further underscore its low-carbon footprint, especially when coupled with renewable energy inputs and co-product recovery systems.

Moving forward, the integration of photoreforming into existing waste management and energy infrastructures could unlock its broader societal benefits. Aligning technology development with supportive policies, such as incentives for clean H_2, carbon credits, and extended producer responsibility schemes, will be essential to drive adoption. Research efforts should prioritize the development of durable, earth-abundant photocatalysts, scalable modular reactors, and hybrid treatment systems that can operate under variable environmental conditions and mixed plastic feedstocks. In general, plastic photoreforming offers more than just a route to clean H_2, it redefines plastic waste as a renewable resource within the framework of a circular economy. With continued interdisciplinary innovation and systems-level thinking, this emerging technology holds strong potential to evolve from a laboratory-scale concept into a commercially viable solution for sustainable energy and environmental remediation.

Author Contributions: Conceptualization, PSS, EMNTE, and TA; validation, PX and HW; resources, PSS and EMNTE; data curation PSS and EMNTE; writing—original draft preparation, PSS and EMNTE; writing—review and editing, PX, TA and HW; visualization, PSS and EMNTE; supervision, PX and HW; project administration, HW; All authors have read and agreed to the published version of the manuscript.

Funding: This research received no external funding.

Conflicts of Interest: The authors declare that they have no affiliations with or involvement in any organization or entity with any financial interest in the subject matter or materials discussed in this manuscript.

References

1. B. Research, "Market Trends in the Plastics Industry: An Analysis of Developments by Key Plastics Manufacturers," Sep 2023 2023. [Online]. Available: https://www.bccresearch.com/market-research/plastics/plastic-industry-market-trends.html
2. G. E. Network. "Plastic Production and Industry | Plastics and the Environment Series." https://www.genevaenvironmentnetwork.org/resources/updates/plastic-production-and-industry/ (accessed.
3. M. Kumar *et al.*, "Current research trends on micro-and nano-plastics as an emerging threat to global environment: A review," *Journal of Hazardous Materials*, vol. 409, p. 124967, 2021.

 doi:10.20944/preprints202504.1506.v1

4. P. Europe. *Plastics – the fast Facts 2024*. (2024). [Online]. Available: https://plasticseurope.org/knowledge-hub/plastics-the-fast-facts-2024/
5. "Department of Energy Hydrogen Program Plan," U.S. Department of Energy 2024. [Online]. Available: https://www.hydrogen.energy.gov/docs/hydrogenprogramlibraries/pdfs/hydrogen-program-plan-2024.pdf?sfvrsn=bfc739dd_1
6. K. Lan and Y. Yao, "Feasibility of gasifying mixed plastic waste for hydrogen production and carbon capture and storage," *Communications Earth & Environment*, vol. 3, no. 1, p. 300, 2022.
7. C. Jehanno *et al.*, "Critical advances and future opportunities in upcycling commodity polymers," *Nature*, vol. 603, no. 7903, pp. 803-814, 2022/03/01 2022, doi: 10.1038/s41586-021-04350-0.
8. U. EPA. "National Overview: Facts and Figures on Materials, Wastes and Recycling." https://www.epa.gov/facts-and-figures-about-materials-waste-and-recycling/national-overview-facts-and-figures-materials#Recycling/Composting (accessed.
9. T. K. Anh Nguyen, T. Trần-Phú, R. Daiyan, X. Minh Chau Ta, R. Amal, and A. Tricoli, "From Plastic Waste to Green Hydrogen and Valuable Chemicals Using Sunlight and Water," *Angewandte Chemie International Edition*, vol. 63, no. 32, p. e202401746, 2024, doi: https://doi.org/10.1002/anie.202401746.
10. E. M. N. T. Edirisooriya, P. S. Senanayake, H. B. Wang, M. R. Talipov, P. Xu, and H. Wang, "Photo-reforming and degradation of waste plastics under UV and visible light for H2 production using nanocomposite photocatalysts," *Journal of Environmental Chemical Engineering*, vol. 11, no. 2, p. 109580, 2023/04/01/ 2023, doi: https://doi.org/10.1016/j.jece.2023.109580.
11. H. T. N. Hai, T. T. Nguyen, M. Nishibori, T. Ishihara, and K. Edalati, "Photoreforming of plastic waste into valuable products and hydrogen using a high-entropy oxynitride with distorted atomic-scale structure," *Applied Catalysis B: Environment and Energy*, vol. 365, p. 124968, 2025/05/15/ 2025, doi: https://doi.org/10.1016/j.apcatb.2024.124968.
12. M. Ashraf, N. Ullah, I. Khan, W. Tremel, S. Ahmad, and M. N. Tahir, "Photoreforming of Waste Polymers for Sustainable Hydrogen Fuel and Chemicals Feedstock: Waste to Energy," *Chemical Reviews*, vol. 123, no. 8, pp. 4443-4509, 2023/04/26 2023, doi: 10.1021/acs.chemrev.2c00602.
13. A. Mehtab *et al.*, "Hydrogen Energy as Sustainable Energy Resource for Carbon-Neutrality Realization," *ACS Sustainable Resource Management*, vol. 1, no. 4, pp. 604-620, 2024/04/25 2024, doi: 10.1021/acssusresmgt.4c00039.
14. L.-H. Chang, S.-T. Yong, S. P. Chai, L. K. Putri, L. L. Tan, and A. R. Mohamed, "A review of methanol photoreforming: elucidating the mechanisms, photocatalysts and recent advancement strategies," *Materials Today Chemistry*, 2023.
15. X. Tang, X. Han, N. H. M. Sulaiman, L. He, and X. Zhou, "Recent Advances in the Photoreforming of Plastic Waste: Principles, Challenges, and Perspectives," *Industrial & Engineering Chemistry Research*, vol. 62, no. 23, pp. 9032-9045, 2023/06/14 2023, doi: 10.1021/acs.iecr.3c00809.
16. C. Y. Toe *et al.*, "Advancing photoreforming of organics: highlights on photocatalyst and system designs for selective oxidation reactions," *Energy & Environmental Science*, vol. 14, no. 3, pp. 1140-1175, 2021, doi: 10.1039/d0ee03116j.
17. S. P. Shelake, D. N. Sutar, B. M. Abraham, T. Banerjee, A. V. S. Sainath, and U. Pal, "Emerging Photoreforming Process to Hydrogen Production: A Future Energy," *Advanced Functional Materials*, vol. 34, no. 40, p. 2403795, 2024, doi: https://doi.org/10.1002/adfm.202403795.
18. E. M. N. Thiloka Edirisooriya, P. S. Senanayake, P. Xu, and H. Wang, "Hydrogen production and value-added chemical recovery from the photo-reforming process using waste plastics," *Journal of Environmental Chemical Engineering*, vol. 11, no. 6, p. 111429, 2023/12/01/ 2023, doi: https://doi.org/10.1016/j.jece.2023.111429.
19. P. Praus, "Photoreforming for microplastics recycling: A critical review," *Journal of Environmental Chemical Engineering*, vol. 12, no. 3, p. 112525, 2024/06/01/ 2024, doi: https://doi.org/10.1016/j.jece.2024.112525.
20. T. K. A. Nguyen *et al.*, "Understanding Structure-Activity Relationship in Pt-loaded g-C3N4 for Efficient Solar- Photoreforming of Polyethylene Terephthalate Plastic and Hydrogen Production," *Small Methods*, vol. 8, no. 2, p. 2300427, 2024, doi: https://doi.org/10.1002/smtd.202300427.

21. X. Li, Q. Wang, Y. Sun, S. Sun, and L. Ge, "Photogenerated charge carriers' regulation strategies: Structure design, mechanism, and characterization technology," *International Journal of Hydrogen Energy*, vol. 69, pp. 1341-1365, 2024/06/05/ 2024, doi: https://doi.org/10.1016/j.ijhydene.2024.05.162.
22. A. S. Morshedy, E. M. El-Fawal, T. Zaki, A. A. El-Zahhar, M. M. Alghamdi, and A. M. A. El Naggar, "A review on heterogeneous photocatalytic materials: Mechanism, perspectives, and environmental and energy sustainability applications," *Inorganic Chemistry Communications*, vol. 163, p. 112307, 2024/05/01/ 2024, doi: https://doi.org/10.1016/j.inoche.2024.112307.
23. N. Goodarzi, Z. Ashrafi-Peyman, E. Khani, and A. Z. Moshfegh, "Recent Progress on Semiconductor Heterogeneous Photocatalysts in Clean Energy Production and Environmental Remediation," *Catalysts*, vol. 13, no. 7, p. 1102, 2023. [Online]. Available: https://www.mdpi.com/2073-4344/13/7/1102.
24. M. B. Tahir and K. N. Riaz, "Fundamentals of Photocatalysis for Environmental Remediation," in *Nanomaterials and Photocatalysis in Chemistry: Mechanistic and Experimental Approaches*, M. B. Tahir and K. N. Riaz Eds. Singapore: Springer Singapore, 2021, pp. 19-41.
25. M. M. Khan, "Chapter 4 - Semiconductors as photocatalysts: visible-light active materials," in *Theoretical Concepts of Photocatalysis*, M. Mansoob Khan Ed.: Elsevier, 2023, pp. 53-75.
26. K. Huang *et al.*, "Interface-induced charge transfer pathway switching of a Cu2O-TiO2 photocatalyst from p-n to S-scheme heterojunction for effective photocatalytic H2 evolution," *Journal of Materials Science & Technology*, vol. 193, pp. 98-106, 2024/09/10/ 2024, doi: https://doi.org/10.1016/j.jmst.2024.01.034.
27. Y. Liu *et al.*, "Bandgap engineering control bifunctional MnxCd1-xS photocatalysts selectively reforming xylose to C3 organic acids and efficient hydrogen production," *Journal of Colloid and Interface Science*, vol. 652, pp. 2066-2075, 2023/12/15/ 2023, doi: https://doi.org/10.1016/j.jcis.2023.09.023.
28. V. S. Mothika, P. Sutar, P. Verma, S. Das, S. K. Pati, and T. K. Maji, "Regulating Charge-Transfer in Conjugated Microporous Polymers for Photocatalytic Hydrogen Evolution," *Chemistry – A European Journal*, vol. 25, no. 15, pp. 3867-3874, 2019, doi: https://doi.org/10.1002/chem.201805478.
29. T. Li and Y. Jing, "Band Structure Engineering of 2D Heterotriangulene Polymers by Incorporating Acetylenic Linkages for Photocatalytic Hydrogen Production," *The Journal of Physical Chemistry C*, vol. 126, no. 42, pp. 17836-17843, 2022/10/27 2022, doi: 10.1021/acs.jpcc.2c04807.
30. N. Tuan Van, T. Mahider, L. Quyet Van, T. Chau Van, A. Sang Hyun, and K. Soo Young, "Recent progress and strategies of non-noble metal electrocatalysts based on MoS₂/MOF for the hydrogen evolution reaction in water electrolysis: an overview," *Microstructures*, vol. 4, no. 4, p. 2024046, 2024, doi: 10.20517/microstructures.2024.24.
31. X. Wang, M. Yu, and X. Feng, "Electronic structure regulation of noble metal-free materials toward alkaline oxygen electrocatalysis," *eScience*, vol. 3, no. 4, p. 100141, 2023/08/01/ 2023, doi: https://doi.org/10.1016/j.esci.2023.100141.
32. J. Ni *et al.*, "Development of noble metal-free electrocatalysts towards acidic water oxidation: From fundamental understanding to state-of-the-art catalysts," *eScience*, vol. 5, no. 2, p. 100295, 2025/03/01/ 2025, doi: https://doi.org/10.1016/j.esci.2024.100295.
33. Y. Lin, Y. Cao, Q. Yao, O. J. H. Chai, and J. Xie, "Engineering Noble Metal Nanomaterials for Pollutant Decomposition," *Industrial & Engineering Chemistry Research*, vol. 59, no. 47, pp. 20561-20581, 2020/11/25 2020, doi: 10.1021/acs.iecr.0c04258.
34. E. M. N. T. Edirisooriya, P. S. Senanayake, P. Xu, and H. Wang, "Enhanced H2 Production Efficiency in Photo-Reforming of PET Waste Plastic Using Dark-Deposited Atom/Nanocomposite Pt/TiO2 Photocatalysts," *Catalysts*, vol. 15, no. 4, p. 334, 2025. [Online]. Available: https://www.mdpi.com/2073-4344/15/4/334.
35. J. Wang, P. Kumar, H. Zhao, M. G. Kibria, and J. Hu, "Polymeric carbon nitride-based photocatalysts for photoreforming of biomass derivatives," *Green Chemistry*, 10.1039/D1GC02307A vol. 23, no. 19, pp. 7435-7457, 2021, doi: 10.1039/D1GC02307A.
36. S. Yue, Z. Zhao, T. Zhang, F. Li, P. Wang, and S. Zhan, "Photoreforming of Plastic Waste to Sustainable Fuels and Chemicals: Waste to Energy," *Environmental Science & Technology*, vol. 58, no. 52, pp. 22865-22879, 2024.

37. A. Gautam, S. Das, and M. I. Ahmad, "Band gap engineering through calcium addition in (Mg, Co, Ni, Cu, Zn)O high entropy oxide for efficient photocatalysis," *Surfaces and Interfaces,* vol. 46, p. 104054, 2024/03/01/ 2024, doi: https://doi.org/10.1016/j.surfin.2024.104054.
38. Y. Yu, Z. Zhu, and H. Huang, "Surface engineered single‐atom systems for energy conversion," *Advanced Materials,* vol. 36, no. 16, p. 2311148, 2024.
39. X. Liang *et al.*, "Photoreforming of poly(ethylene-terephthalate) plastic into valuable chemicals and hydrogen over BiVO4/MoOx: Synergistic promotion of oxidation and reduction processes," *Applied Catalysis B: Environment and Energy,* vol. 357, p. 124326, 2024/11/15/ 2024, doi: https://doi.org/10.1016/j.apcatb.2024.124326.
40. X. Zhang, W. Zu, and L. Y. S. Lee, "Crucial role of pre-treatment in plastic photoreforming for precision upcycling," *npj Materials Sustainability,* vol. 3, no. 1, p. 3, 2025/01/16 2025, doi: 10.1038/s44296-024-00045-5.
41. J. Xiao, "Catalyzing photo-degradation of waste plastics with a uranium complex," *Science Bulletin,* vol. 68, no. 21, pp. 2498-2499, 2023, doi: https://doi.org/10.1016/j.scib.2023.08.045.
42. B. Gewert, M. M. Plassmann, and M. MacLeod, "Pathways for degradation of plastic polymers floating in the marine environment," *Environmental Science: Processes & Impacts,* vol. 17, no. 9, pp. 1513-1521, 2015, doi: https://doi.org/10.1039/C5EM00207A.
43. G. Scott, *Degradable Polymers: Principles and Applications*. 2002.
44. G. Pritchard, *Plastics Additives*. Springer Dordrecht, 1998.
45. L. H. Sperling, *Introduction to Physical Polymer Science*. Hoboken, New Jersey: John Wiley & Sons, Inc. , 2006.
46. S. A. Norman, E. Michael, M. Mehrdad, and J. Ken, "Hydrolytic degradation of poly(ethylene terephthalate): Importance of chain scission versus crystallinity," *European Polymer Journal,* vol. 27, no. 12, pp. 1373-1378, 1991, doi: https://doi.org/10.1016/0014-3057(91)90237-I.
47. J. K. Fink, Thomas, S., Visakh, P. M., *Handbook of Engineering and Specialty Thermoplastics*. WILEY, 2011.
48. T. Uekert, M. F. Kuehnel, D. W. Wakerley, and E. Reisner, "Plastic waste as a feedstock for solar-driven H2 generation," *Energy & Environmental Science,* vol. 11, no. 10, pp. 2853-2857, 2018, doi: https://doi.org/10.1039/C8EE01408F.
49. E. M. N. T. Edirisooriya, S. S. Punhasa, X. Pei, and W. Huiyao, "Hydrogen production and value-added chemical recovery from the photo-reforming process using waste plastics," *Journal of Environmental Chemical Engineering,* vol. 11, no. 6, p. 111429, 2023, doi: https://doi.org/10.1016/j.jece.2023.111429.
50. X. Jiao, K. Zheng, Z. Hu, S. Zhu, Y. Sun, and Y. Xie, "Conversion of waste plastics into value‐added carbonaceous fuels under mild conditions," *Advanced Materials,* vol. 33, no. 50, p. 2005192, 2021, doi: https://doi.org/10.1002/adma.202005192.
51. X. Jiao, K. Zheng, Z. Hu, S. Zhu, Y. Sun, and Y. Xie, "Conversion of Waste Plastics into Value-Added Carbonaceous Fuels under Mild Conditions," *Advanced Materials,* vol. 33, no. 50, p. 2005192, 2021, doi: https://doi.org/10.1002/adma.202005192.
52. S. Bhattacharjee, V. Andrei, C. Pornrungroj, M. Rahaman, C. M. Pichler, and E. Reisner, "Reforming of Soluble Biomass and Plastic Derived Waste Using a Bias-Free Cu30Pd70|Perovskite|Pt Photoelectrochemical Device," *Advanced Functional Materials,* vol. 32, no. 7, p. 2109313, 2022, doi: https://doi.org/10.1002/adfm.202109313.
53. M. Rakowski DuBois and D. L. DuBois, "Development of molecular electrocatalysts for CO2 reduction and H2 production/oxidation," (in eng), *Acc Chem Res,* vol. 42, no. 12, pp. 1974-82, Dec 21 2009, doi: 10.1021/ar900110c.
54. X. Zhang, W. Zu, and L. Y. S. Lee, "Crucial role of pre-treatment in plastic photoreforming for precision upcycling," *npj Materials Sustainability,* vol. 3, no. 1, 2025, doi: 10.1038/s44296-024-00045-5.
55. S. Yue, Z. Zhao, T. Zhang, F. Li, P. Wang, and S. Zhan, "Photoreforming of Plastic Waste to Sustainable Fuels and Chemicals: Waste to Energy," *Environ Sci Technol,* vol. 58, no. 52, pp. 22865-22879, Dec 31 2024, doi: 10.1021/acs.est.4c06688.
56. T. Uekert, H. Kasap, and E. Reisner, "Photoreforming of Nonrecyclable Plastic Waste over a Carbon Nitride/Nickel Phosphide Catalyst," *Journal of the American Chemical Society,* vol. 141, no. 38, pp. 15201-15210, 2019/09/25 2019, doi: 10.1021/jacs.9b06872.

 doi:10.20944/preprints202504.1506.v1

57. Y. Wan *et al.*, "Enhanced degradation of polyethylene terephthalate plastics by CdS/CeO2 heterojunction photocatalyst activated peroxymonosulfate," *Journal of Hazardous Materials,* vol. 452, p. 131375, 2023/06/15/ 2023, doi: https://doi.org/10.1016/j.jhazmat.2023.131375.
58. F. Ippolito, G. Hübner, T. Claypole, and P. Gane, "Calcium Carbonate as Functional Filler in Polyamide 12-Manipulation of the Thermal and Mechanical Properties," *Processes,* vol. 9, no. 6, p. 937, 2021. [Online]. Available: https://www.mdpi.com/2227-9717/9/6/937.
59. S. Siraj, A. H. Al-Marzouqi, M. Z. Iqbal, and W. Ahmed, "Impact of Micro Silica Filler Particle Size on Mechanical Properties of Polymeric Based Composite Material," (in eng), *Polymers (Basel),* vol. 14, no. 22, Nov 9 2022, doi: 10.3390/polym14224830.
60. C. Cazan, A. Enesca, and L. Andronic, "Synergic Effect of TiO(2) Filler on the Mechanical Properties of Polymer Nanocomposites," (in eng), *Polymers (Basel),* vol. 13, no. 12, Jun 20 2021, doi: 10.3390/polym13122017.
61. G. L. Chiarello, A. Di Paola, L. Palmisano, and E. Selli, "Effect of titanium dioxide crystalline structure on the photocatalytic production of hydrogen," *Photochemical & Photobiological Sciences,* 10.1039/C0PP00154F vol. 10, no. 3, pp. 355-360, 2011, doi: 10.1039/C0PP00154F.
62. Y. Miao, Y. Zhao, J. Gao, J. Wang, and T. Zhang, "Direct Photoreforming of Real-World Polylactic Acid Plastics into Highly Selective Value-Added Pyruvic Acid under Visible Light," *Journal of the American Chemical Society,* vol. 146, no. 7, pp. 4842-4850, 2024/02/21 2024, doi: 10.1021/jacs.3c13000.
63. H. Li, B. Cheng, J. Xu, J. Yu, and S. Cao, "Crystalline carbon nitrides for photocatalysis," *EES Catalysis,* vol. 2, no. 2, pp. 411-447, 2024, doi: 10.1039/d3ey00302g.
64. T. K. Anh Nguyen, T. Tran-Phu, R. Daiyan, X. Minh Chau Ta, R. Amal, and A. Tricoli, "From Plastic Waste to Green Hydrogen and Valuable Chemicals Using Sunlight and Water," *Angew Chem Int Ed Engl,* vol. 63, no. 32, p. e202401746, Aug 5 2024, doi: 10.1002/anie.202401746.
65. H. Nagakawa and M. Nagata, "Photoreforming of Organic Waste into Hydrogen Using a Thermally Radiative CdO(x)/CdS/SiC Photocatalyst," *ACS Appl Mater Interfaces,* vol. 13, no. 40, pp. 47511-47519, Oct 13 2021, doi: 10.1021/acsami.1c11888.
66. E. M. N. T. Edirisooriya, P. S. Senanayake, P. Xu, M. R. Talipov, and H. Wang, "Optimization of green hydrogen evolution from low-density plastics using TiO2-based nano-photocatalysts with techno-economic and carbon footprint assessment," *Nanotechnology for Environmental Engineering,* vol. 9, no. 4, pp. 817-832, 2024/12/01 2024, doi: 10.1007/s41204-024-00397-2.
67. H. Pan, J. Li, Y. Wang, Q. Xia, L. Qiu, and B. Zhou, "Solar-Driven Biomass Reforming for Hydrogen Generation: Principles, Advances, and Challenges," (in eng), *Adv Sci (Weinh),* vol. 11, no. 29, p. e2402651, Aug 2024, doi: 10.1002/advs.202402651.
68. D. N. Sutar, S. P. Shelake, N. R. Indla, S. Varangane, A. V. Sesha Sainath, and U. Pal, "Visible light-driven photoreforming of polystyrene segmented glycopolymer architectures for enhanced hydrogen generation," *Materials Today Energy,* vol. 45, p. 101667, 2024/10/01/ 2024, doi: https://doi.org/10.1016/j.mtener.2024.101667.
69. J. He *et al.*, "Efficient photodegradation of polystyrene microplastics integrated with hydrogen evolution: Uncovering degradation pathways," *iScience,* vol. 26, no. 6, p. 106833, 2023/06/16/ 2023, doi: https://doi.org/10.1016/j.isci.2023.106833.
70. L. Lan *et al.*, "Effect of Ball-Milling Pretreatment of Cellulose on Its Photoreforming for H(2) Production," (in eng), *ACS Sustain Chem Eng,* vol. 10, no. 15, pp. 4862-4871, Apr 18 2022, doi: 10.1021/acssuschemeng.1c07301.
71. M. Samadi, M. Zirak, A. Naseri, E. Khorashadizade, and A. Z. Moshfegh, "Recent progress on doped ZnO nanostructures for visible-light photocatalysis," *Thin Solid Films,* vol. 605, pp. 2-19, 2016/04/30/ 2016, doi: https://doi.org/10.1016/j.tsf.2015.12.064.
72. M. A. Khan, S. Mutahir, I. Shaheen, Y. Qunhui, M. Bououdina, and M. Humayun, "Recent advances over the doped g-C3N4 in photocatalysis: A review," *Coordination Chemistry Reviews,* vol. 522, p. 216227, 2025/01/01/ 2025, doi: https://doi.org/10.1016/j.ccr.2024.216227.

 doi:10.20944/preprints202504.1506.v1

73. J. R. Wang *et al.*, "Robust links in photoactive covalent organic frameworks enable effective photocatalytic reactions under harsh conditions," *Nat Commun,* vol. 15, no. 1, p. 1267, Feb 10 2024, doi: 10.1038/s41467-024-45457-y.
74. N. Sun, X. Si, L. He, J. Zhang, and Y. Sun, "Strategies for enhancing the photocatalytic activity of semiconductors," *International Journal of Hydrogen Energy,* vol. 58, pp. 1249-1265, 2024/03/08/ 2024, doi: https://doi.org/10.1016/j.ijhydene.2024.01.319.
75. H. M. Rasheed, K. Aroosh, D. Meng, X. Ruan, M. Akhter, and X. Cui, "A review on modified ZnO to address environmental challenges through photocatalysis: Photodegradation of organic pollutants," *Materials Today Energy,* vol. 48, p. 101774, 2025/03/01/ 2025, doi: https://doi.org/10.1016/j.mtener.2024.101774.
76. J. Jeyavani, K. A. Al-Ghanim, M. Govindarajan, G. Malafaia, and B. Vaseeharan, "A convenient strategy for mitigating microplastics in wastewater treatment using natural light and ZnO nanoparticles as photocatalysts: A mechanistic study," *Journal of Contaminant Hydrology,* vol. 267, p. 104436, 2024/11/01/ 2024, doi: https://doi.org/10.1016/j.jconhyd.2024.104436.
77. Y. Ma, G. Hai, J. Liu, J. Bao, Y. Li, and G. Wang, "Enhanced visible light photocatalytic hydrogen evolution by intimately contacted Ni2P decorated Ni-doped CdS nanospheres," *Chemical Engineering Journal,* vol. 441, p. 136002, 2022/08/01/ 2022, doi: https://doi.org/10.1016/j.cej.2022.136002.
78. N. Downs, Parisi, A.V., Galligan, L., Turner, J., Amar, A., King, R., Ultra, F., & Butler, H., "Solar radiation and the UV index: An application of numerical integration, trigonometric functions, online education and the modelling process," *International Journal of Research in Education and Science,* vol. 2, no. 1, pp. 179-189, 2016.
79. J. D. Graham and N. I. Hammer, "Photocatalytic Water Splitting and Carbon Dioxide Reduction," in *Handbook of Climate Change Mitigation*, W.-Y. Chen, J. Seiner, T. Suzuki, and M. Lackner Eds. New York, NY: Springer US, 2012, pp. 1755-1780.
80. W. Ma, L. Yu, P. Kang, Z. Chu, and Y. Li, "Modifications and Applications of Metal-Organic-Framework-Based Materials for Photocatalysis," *Molecules,* vol. 29, no. 24, Dec 11 2024, doi: 10.3390/molecules29245834.
81. H. Zhang, C. Li, Y. Li, J. Pang, and X. Bu, "The Advanced Synthesis of MOFs-Based Materials in Photocatalytic HER in Recent Three Years," *Catalysts,* vol. 12, no. 11, 2022, doi: 10.3390/catal12111350.
82. Q. Wang *et al.*, "Recent Advances in g-C(3)N(4)-Based Materials and Their Application in Energy and Environmental Sustainability," *Molecules,* vol. 28, no. 1, Jan 3 2023, doi: 10.3390/molecules28010432.
83. J. Y. Kim and D. H. Youn, "Nanomaterials for Advanced Photocatalytic Plastic Conversion," *Molecules,* vol. 28, no. 18, Sep 7 2023, doi: 10.3390/molecules28186502.
84. T. T. Nguyen, J. Hidalgo-Jiménez, X. Sauvage, K. Saito, Q. Guo, and K. Edalati, "Phase and sulfur vacancy engineering in cadmium sulfide for boosting hydrogen production from catalytic plastic waste photoconversion," *Chemical Engineering Journal,* vol. 504, p. 158730, 2025/01/15/ 2025, doi: https://doi.org/10.1016/j.cej.2024.158730.
85. M. A. Ahmed, S. A. Mahmoud, and A. A. Mohamed, "Unveiling the photocatalytic potential of graphitic carbon nitride (g-C(3)N(4)): a state-of-the-art review," *RSC Adv,* vol. 14, no. 35, pp. 25629-25662, Aug 12 2024, doi: 10.1039/d4ra04234d.
86. L. T. Zongyang Ya, Dong Xu, Hua Wang, Shengbo Zhang, "Photoreforming of waste plastic by B-doped carbon nitride nanotube: Atomic-level modulation and mechanism insights," *American Institute of Chemical Engineers,* 2025, doi: https://doi.org/10.1002/aic.18740.
87. J.-Q. Yan, D.-W. Sun, and J.-H. Huang, "Synergistic poly(lactic acid) photoreforming and H2 generation over ternary NixCo1-xP/reduced graphene oxide/g-C3N4 composite," *Chemosphere,* vol. 286, p. 131905, 2022/01/01/ 2022, doi: https://doi.org/10.1016/j.chemosphere.2021.131905.
88. D. Liu, J. Yao, S. Chen, J. Zhang, R. Li, and T. Peng, "Construction of rGO-coupled C3N4/C3N5 2D/2D Z-scheme heterojunction to accelerate charge separation for efficient visible light H2 evolution," *Applied Catalysis B: Environmental,* vol. 318, p. 121822, 2022/12/05/ 2022, doi: https://doi.org/10.1016/j.apcatb.2022.121822.
89. S. Chen, T. Takata, and K. Domen, "Particulate photocatalysts for overall water splitting," *Nature Reviews Materials,* vol. 2, no. 10, p. 17050, 2017/08/01 2017, doi: 10.1038/natrevmats.2017.50.

90. Z. Xi, "Nanostructures Design: the Role of Cocatalysts for Hydrogen and Oxygen Generation in Photocatalytic Water Splitting," *arXiv: Chemical Physics*, 2021.
91. O. Al-Madanat, Y. AlSalka, W. Ramadan, and D. W. Bahnemann, "TiO2 Photocatalysis for the Transformation of Aromatic Water Pollutants into Fuels," *Catalysts*, vol. 11, no. 3, 2021, doi: 10.3390/catal11030317.
92. K. S. Exner, "On the optimum binding energy for the hydrogen evolution reaction: How do experiments contribute?," *Electrochemical Science Advances*, vol. 2, no. 4, 2021, doi: 10.1002/elsa.202100101.
93. G. Cha *et al.*, "As a single atom Pd outperforms Pt as the most active co-catalyst for photocatalytic H2 evolution," *iScience*, vol. 24, no. 8, p. 102938, 2021/08/20/ 2021, doi: https://doi.org/10.1016/j.isci.2021.102938.
94. A. Chen, M.-Q. Yang, S. Wang, and Q. Qian, "Recent Advancements in Photocatalytic Valorization of Plastic Waste to Chemicals and Fuels," *Frontiers in Nanotechnology*, vol. 3, 2021, doi: 10.3389/fnano.2021.723120.
95. Y. Chen, L. Bai, D. Peng, X. Wang, M. Wu, and Z. Bian, "Advancements in catalysis for plastic resource utilization," *Environmental Science: Advances*, vol. 2, no. 9, pp. 1151-1166, 2023, doi: 10.1039/d3va00158j.
96. Y. Pan, Y. Lin, Y. Chen, Y. Liu, and C. Liu, "Cobalt phosphide-based electrocatalysts: synthesis and phase catalytic activity comparison for hydrogen evolution," *Journal of Materials Chemistry A*, vol. 4, no. 13, pp. 4745-4754, 2016, doi: 10.1039/c6ta00575f.
97. S. Chu *et al.*, "Photocatalytic Conversion of Plastic Waste: From Photodegradation to Photosynthesis," *Advanced Energy Materials*, vol. 12, no. 22, 2022, doi: 10.1002/aenm.202200435.
98. B. Mokhtar, M. G. Ahmed, H. S. Alqahtani, and T. A. Kandiel, "Biomass and Plastic Photoreforming for Hydrogen and Valuable Chemicals Production." Berlin, Heidelberg: Springer Berlin Heidelberg, pp. 1-31.
99. M. T. Islam *et al.*, "Selectivity of Sol-Gel and Hydrothermal TiO(2) Nanoparticles towards Photocatalytic Degradation of Cationic and Anionic Dyes," *Molecules*, vol. 28, no. 19, Sep 27 2023, doi: 10.3390/molecules28196834.
100. A. B. Quispe Cohaila *et al.*, "Improving Photocatalytic Hydrogen Production with Sol–Gel Prepared $NiTiO_3/TiO_2$ Composite," *Energies*, vol. 17, no. 23, 2024, doi: 10.3390/en17235830.
101. N. Kadiyala *et al.*, "Ionic Liquid Mediated Sol Gel Method for Fabrication of Nanostructured Cerium and Phosphorus Doped TiO(2) - A Benign Photocatalyst: Diversified Applications in Degradation of Dyes and Microbes," (in eng), *ACS Omega*, vol. 10, no. 3, pp. 2658-2678, Jan 28 2025, doi: 10.1021/acsomega.4c07743.
102. M. T. Islam *et al.*, "Selectivity of Sol-Gel and Hydrothermal TiO2 Nanoparticles towards Photocatalytic Degradation of Cationic and Anionic Dyes," *Molecules*, vol. 28, no. 19, p. 6834, 2023. [Online]. Available: https://www.mdpi.com/1420-3049/28/19/6834.
103. F. Xu *et al.*, "One-Step Hydrothermal Synthesis of Nanostructured MgBi(2)O(6)/TiO(2) Composites for Enhanced Hydrogen Production," (in eng), *Nanomaterials (Basel)*, vol. 12, no. 8, Apr 11 2022, doi: 10.3390/nano12081302.
104. A. Zindrou, P. Psathas, and Y. Deligiannakis, "Flame Spray Pyrolysis Synthesis of Vo-Rich Nano-SrTiO3-x," *Nanomaterials*, vol. 14, no. 4, p. 346, 2024. [Online]. Available: https://www.mdpi.com/2079-4991/14/4/346.
105. S. K. Nayak *et al.*, "Metal–Organic Framework-Derived Hierarchical Ag/Sr6Bi2O9-α-Bi2O3 Ternary Photocatalyst for Micropollutant Remediation and Bacterial Photoinactivation," *ACS Applied Engineering Materials*, vol. 2, no. 1, pp. 179-194, 2024/01/26 2024, doi: 10.1021/acsaenm.3c00710.
106. C. Wang and M. N. Ghazzal, "Nanostructured TiO2for improving the solar-to-hydrogen conversion efficiency," *Energy Advances*, vol. 2, no. 7, pp. 965-979, 2023, doi: 10.1039/d3ya00089c.
107. Y. Abdel-Maksoud, E. Imam, and A. Ramadan, "TiO2 Solar Photocatalytic Reactor Systems: Selection of Reactor Design for Scale-up and Commercialization—Analytical Review," *Catalysts*, vol. 6, no. 9, 2016, doi: 10.3390/catal6090138.
108. R. A. Damodar, S.-J. You, and S.-H. Ou, "Coupling of membrane separation with photocatalytic slurry reactor for advanced dye wastewater treatment," *Separation and Purification Technology*, vol. 76, no. 1, pp. 64-71, 2010, doi: 10.1016/j.seppur.2010.09.021.
109. W. Xi and S.-u. Geissen, "Separation of titanium dioxide from photocatalytically treated water by cross-flow microfiltration," *Water Research*, vol. 35, no. 5, pp. 1256-1262, 2001/04/01/ 2001, doi: https://doi.org/10.1016/S0043-1354(00)00378-X.

 doi:10.20944/preprints202504.1506.v1

110. H. Jiang, G. Zhang, T. Huang, J. Chen, Q. Wang, and Q. Meng, "Photocatalytic membrane reactor for degradation of acid red B wastewater," *Chemical Engineering Journal,* vol. 156, no. 3, pp. 571-577, 2010/02/01/ 2010, doi: https://doi.org/10.1016/j.cej.2009.04.011.
111. R. Yang, J. Xu, J. Wu, D. Lu, F. Wang, and K. Nie, "Enzyme Immobilization on Stainless Steel Fleece and Its Mass Transfer Enhancement of Enzymatic Catalysis in a Rotating Packed Bed Reactor," *Catalysts,* vol. 13, no. 12, 2023, doi: 10.3390/catal13121501.
112. S. E. Kudaibergenov and G. I. Dzhardimalieva, "Flow-Through Catalytic Reactors Based on Metal Nanoparticles Immobilized within Porous Polymeric Gels and Surfaces/Hollows of Polymeric Membranes," *Polymers (Basel),* vol. 12, no. 3, Mar 4 2020, doi: 10.3390/polym12030572.
113. F. Khodadadian, "Optimizing photon utilization in LED-based photocatalytic reactors," PhD, Delft University of Technology, Dissertation (TU Delft), Delft University of Technology, 2019. [Online]. Available: https://resolver.tudelft.nl/uuid:68bc7aa0-914c-4d2d-8e32-9d0ef996fdcc
114. H. Fu *et al.*, "Green hydrogen production via a photocatalyst-enabled optical fiber system: A promising route to net-zero emissions," *Energy and Climate Change,* vol. 6, p. 100175, 2025/12/01/ 2025, doi: https://doi.org/10.1016/j.egycc.2025.100175.
115. P. P. Kant, "Optimizing photocatalysts and photoreactors for solar fuel synthesis," PhD, Faculty of Chemical and Process Engineering Institute of Micro Process Engineering 2023. [Online]. Available: https://publikationen.bibliothek.kit.edu/1000162170
116. S. N. Degerli, A. Gramegna, M. Tommasi, G. Ramis, and I. Rossetti, "Reactor and Plant Designs for the Solar Photosynthesis of Fuels," *Energies,* vol. 17, no. 13, p. 3112, 2024. [Online]. Available: https://www.mdpi.com/1996-1073/17/13/3112.
117. G. B. Ramis, E.; Rossetti, I, "Photoreactors Design for Hydrogen Production," *Chem. Eng. Trans.*, vol. 74, pp. 481–486, 2019, doi: 10.3303/CET1974081.
118. N. F. Jaafar, Jalil, A. A., Triwahyono, S., & Ripin, A. , "Significant Effect of pH on Photocatalytic Degradation of Organic Pollutants Using Semiconductor Catalysts.," *Jurnal Teknologi,* vol. 78, pp. 7-12, 2016, doi: DOI: 10.11113/jt.v78.9559.
119. F. Azeez *et al.*, "The effect of surface charge on photocatalytic degradation of methylene blue dye using chargeable titania nanoparticles," (in eng), *Sci Rep,* vol. 8, no. 1, p. 7104, May 8 2018, doi: 10.1038/s41598-018-25673-5.
120. J. Wenk, C. Graf, M. Aeschbacher, M. Sander, and S. Canonica, "Effect of Solution pH on the Dual Role of Dissolved Organic Matter in Sensitized Pollutant Photooxidation," *Environmental Science & Technology,* vol. 55, no. 22, pp. 15110-15122, 2021/11/16 2021, doi: 10.1021/acs.est.1c03301.
121. A. Chaudhuri, S. D. A. Zondag, J. H. A. Schuurmans, J. van der Schaaf, and T. Noël, "Scale-Up of a Heterogeneous Photocatalytic Degradation Using a Photochemical Rotor–Stator Spinning Disk Reactor," *Organic Process Research & Development,* vol. 26, no. 4, pp. 1279-1288, 2022/04/15 2022, doi: 10.1021/acs.oprd.2c00012.
122. J. C. García-Prieto, L. A. González-Burciaga, J. B. Proal-Nájera, and M. García-Roig, "Study of Influence Factors in the Evaluation of the Performance of a Photocatalytic Fibre Reactor (TiO2/SiO2) for the Removal of Organic Pollutants from Water," *Catalysts,* vol. 12, no. 2, p. 122, 2022. [Online]. Available: https://www.mdpi.com/2073-4344/12/2/122.
123. J. Akach, J. Kabuba, and A. Ochieng, "Simulation of the Light Distribution in a Solar Photocatalytic Bubble Column Reactor Using the Monte Carlo Method," *Industrial & Engineering Chemistry Research,* vol. 59, no. 40, pp. 17708-17719, 2020/10/07 2020, doi: 10.1021/acs.iecr.0c02124.
124. Q. Jamil, B. Žener, U. Putar, and L. Matoh, "Continuous flow photocatalytic reactor for degradation of selected pollutants: Modeling, kinetics, mineralization rate, and toxicity assessment," *Heliyon,* vol. 10, no. 21, 2024, doi: 10.1016/j.heliyon.2024.e40019.
125. N. H. M. Sulaiman, S. Wang, H. Yue, J. Wei, P. Schmuki, and X. Zhou, "Hydrogen evolution using alloyed AuPd/TiO2 hollow spheres by photoreforming of polyethylene terephthalate waste," *Journal of Materials Chemistry A,* 10.1039/D5TA00189G 2025, doi: 10.1039/D5TA00189G.
126. Y. Zheng *et al.*, "Visible light driven reform of wasted plastics to generate green hydrogen over mesoporous ZnIn(2)S(4)," *RSC Adv,* vol. 13, no. 19, pp. 12663-12669, Apr 24 2023, doi: 10.1039/d3ra02279j.

 doi:10.20944/preprints202504.1506.v1

127. Q. Zhang *et al.*, "Accelerating photocatalytic hydrogen production by anchoring Pt single atoms on few-layer g-C3N4 nanosheets with Pt–N coordination," *Journal of Materials Chemistry C,* 10.1039/D3TC04673G vol. 12, no. 10, pp. 3437-3449, 2024, doi: 10.1039/D3TC04673G.
128. J. Ran *et al.*, "NiPS(3) ultrathin nanosheets as versatile platform advancing highly active photocatalytic H(2) production," *Nat Commun,* vol. 13, no. 1, p. 4600, Aug 6 2022, doi: 10.1038/s41467-022-32256-6.
129. J. Li, H.-P. Ma, G. Zhao, G. Huang, W. Sun, and C. Peng, "Plastic Waste Conversion by Leveraging Renewable Photo/Electro-Catalytic Technologies," *ChemSusChem,* vol. 17, no. 10, p. e202301352, 2024, doi: https://doi.org/10.1002/cssc.202301352.
130. Y. Zheng *et al.*, "Visible light driven reform of wasted plastics to generate green hydrogen over mesoporous ZnIn2S4," *RSC Advances,* 10.1039/D3RA02279J vol. 13, no. 19, pp. 12663-12669, 2023, doi: 10.1039/D3RA02279J.
131. Y. Wan, H. Wang, and P. Huo, "Plastic Degradation and Conversion by Photocatalysis," in *Plastic Degradation and Conversion by Photocatalysis (Volume 2): From Waste to Wealth*, vol. 1490, (ACS Symposium Series, no. 1490): American Chemical Society, 2024, ch. 1, pp. 1-22.
132. N. Qin, A. Mao, J. Zou, L. Mi, and L. Wu, "Visible-light-driven H2 production from heterostructured Zn0.5Cd0.5S–TiO2 photocatalysts modified with reduced graphene oxides," *New Journal of Chemistry,* 10.1039/D1NJ04195A vol. 45, no. 45, pp. 21415-21422, 2021, doi: 10.1039/D1NJ04195A.
133. S. Zhang *et al.*, "Boosted Photoreforming of Plastic Waste via Defect-Rich NiPS3 Nanosheets," *Journal of the American Chemical Society,* vol. 145, no. 11, pp. 6410-6419, 2023/03/22 2023, doi: 10.1021/jacs.2c13590.
134. J. Xu *et al.*, "Plastics-to-syngas photocatalysed by Co–Ga2O3 nanosheets," *National Science Review,* vol. 9, no. 9, p. nwac011, 2022, doi: 10.1093/nsr/nwac011.
135. M. Nees, M. Adeel, L. Pazdur, M. Porters, C. M. L. Vande Velde, and P. Billen, "Polyurethane Waste Recycling: Thermolysis of the Carbamate Fraction," (in eng), *ACS Omega,* vol. 9, no. 43, pp. 43438-43446, Oct 29 2024, doi: 10.1021/acsomega.4c04671.
136. S. Fawzi, E. Yousif, K. Zainulabdeen, M. Bufaroosha, and D. Ahmed, "Highly effective photostabilization of polyvinyl chloride films using omeprazole-tin additive complexes," *Journal of Umm Al-Qura University for Applied Sciences,* 2025/01/11 2025, doi: 10.1007/s43994-024-00207-0.
137. R. Yang, H. Cao, H. Dong, and X. Wang, "The mechanism of UV accelerated aging of polyvinyl chloride in marine environment: The role of free radicals," *Marine Pollution Bulletin,* vol. 207, p. 116736, 2024/10/01/ 2024, doi: https://doi.org/10.1016/j.marpolbul.2024.116736.
138. D. Zhang, C. Zhang, G. Zhao, Y. Gao, T. Zhuang, and Z. Lv, "Single-atom Pt supported on defective graphitic carbon nitride for efficient photocatalytic hydrogen production," *Chemical Engineering Journal,* vol. 505, p. 159567, 2025/02/01/ 2025, doi: https://doi.org/10.1016/j.cej.2025.159567.
139. Y. Jiang *et al.*, "An Integrated Plasma–Photocatalytic System for Upcycling of Polyolefin Plastics," *ChemSusChem,* vol. 16, no. 14, p. e202300106, 2023, doi: https://doi.org/10.1002/cssc.202300106.
140. S. Bhattacharjee *et al.*, "Chemoenzymatic Photoreforming: A Sustainable Approach for Solar Fuel Generation from Plastic Feedstocks," *Journal of the American Chemical Society,* vol. 145, no. 37, pp. 20355-20364, 2023/09/20 2023, doi: https://doi.org/10.1021/jacs.3c05486.
141. K. S. Ng and A. N. Phan, "Evaluating the Techno-economic Potential of an Integrated Material Recovery and Waste-to-Hydrogen System," *Resources, Conservation and Recycling,* vol. 167, p. 105392, 2021/04/01/ 2021, doi: https://doi.org/10.1016/j.resconrec.2020.105392.
142. Z. Chen, W. Wei, X. Chen, Y. Liu, Y. Shen, and B.-J. Ni, "Upcycling of plastic wastes for hydrogen production: Advances and perspectives," *Renewable and Sustainable Energy Reviews,* vol. 195, p. 114333, 2024/05/01/ 2024, doi: https://doi.org/10.1016/j.rser.2024.114333.
143. D. Gunawan *et al.*, "Materials Advances in Photocatalytic Solar Hydrogen Production: Integrating Systems and Economics for a Sustainable Future," *Advanced Materials,* vol. 36, no. 42, p. 2404618, 2024, doi: https://doi.org/10.1002/adma.202404618.
144. D. Ouyang *et al.*, "Light-driven lignocellulosic biomass conversion for production of energy and chemicals," (in eng), *iScience,* vol. 25, no. 10, p. 105221, Oct 21 2022, doi: 10.1016/j.isci.2022.105221.

145. J. Tian, C. Guan, H. Hu, E. Liu, and D. Yang, "Waste plastics promoted photocatalytic H2 evolution over S-scheme NiCr2O4/twinned-Cd0.5Zn0.5S homo-heterojunction," *Acta Physico-Chimica Sinica,* vol. 41, no. 6, p. 100068, 2025/06/01/ 2025, doi: https://doi.org/10.1016/j.actphy.2025.100068.
146. R. Balu, N. K. Dutta, and N. Roy Choudhury, "Plastic Waste Upcycling: A Sustainable Solution for Waste Management, Product Development, and Circular Economy," (in eng), *Polymers (Basel),* vol. 14, no. 22, Nov 8 2022, doi: 10.3390/polym14224788.
147. A. Bratovcic, "Photocatalytic Degradation of Plastic Waste: Recent Progress and Future Perspectives," *Advances in Nanoparticles,* vol. 13, no. 03, pp. 61-78, 2024, doi: 10.4236/anp.2024.133005.
148. G. Biale *et al.*, "A Systematic Study on the Degradation Products Generated from Artificially Aged Microplastics," *Polymers,* vol. 13, no. 12, p. 1997, 2021. [Online]. Available: https://www.mdpi.com/2073-4360/13/12/1997.
149. T. Li, A. Vijeta, C. Casadevall, A. S. Gentleman, T. Euser, and E. Reisner, "Bridging Plastic Recycling and Organic Catalysis: Photocatalytic Deconstruction of Polystyrene via a C–H Oxidation Pathway," *ACS Catalysis,* vol. 12, no. 14, pp. 8155-8163, 2022/07/15 2022, doi: 10.1021/acscatal.2c02292.
150. D. Chu *et al.*, "Photocatalytic Oxidation of Polyethylene to Dicarboxylic Acid over BiOI/BiVO₄ p–n Heterojunction Under Visible Light," *CCS Chemistry,* vol. 0, no. 0, pp. 1-11, doi: doi:10.31635/ccschem.025.202405274.
151. J. P. d. Costa, A. Avellan, C. Mouneyrac, A. Duarte, and T. Rocha-Santos, "Plastic additives and microplastics as emerging contaminants: Mechanisms and analytical assessment," *TrAC Trends in Analytical Chemistry,* vol. 158, p. 116898, 2023/01/01/ 2023, doi: https://doi.org/10.1016/j.trac.2022.116898.
152. X. Zhang, M. Jun, W. Zu, M. Kim, K. Lee, and L. Y. S. Lee, "Photoreforming of Microplastics: Challenges and Opportunities for Sustainable Environmental Remediation," *Small,* vol. 20, no. 46, p. e2403347, Nov 2024, doi: 10.1002/smll.202403347.
153. M. V. S. Maria Vittoria Diamanti, MariaPia Pedeferri, and R. R. Anna Maria Ferrari, *and Daniela Meroni, "Toward Sustainable Photocatalysis: Addressing Deactivation and Environmental Impact of Anodized and Sol–Gel Photocatalysts," 2025, doi: 10.1002/adsu.202401017.
154. Y. He, A. U. Rehman, M. Xu, C. A. Not, A. M. C. Ng, and A. B. Djurišić, "Photocatalytic degradation of different types of microplastics by TiO(x)/ZnO tetrapod photocatalysts," (in eng), *Heliyon,* vol. 9, no. 11, p. e22562, Nov 2023, doi: 10.1016/j.heliyon.2023.e22562.
155. L. V. Bora, M. Bhatt, A. Patel, and N. V. Bora, "Plastic Degradation by Photocatalysis: Basic Concepts and General Mechanisms," in *Plastic Degradation and Conversion by Photocatalysis (Volume 1): A Sustainable Approach*, vol. 1489, (ACS Symposium Series, no. 1489): American Chemical Society, 2024, ch. 1, pp. 1-22.
156. J. Zhao *et al.*, "Highly selective upcycling of plastic mixture waste by microwave-assisted catalysis over Zn/b-ZnO," *Nat Commun,* vol. 16, no. 1, p. 1726, Feb 18 2025, doi: 10.1038/s41467-024-55584-1.
157. H. Du, Y. Xie, and J. Wang, "Microplastic degradation methods and corresponding degradation mechanism: Research status and future perspectives," *Journal of Hazardous Materials,* vol. 418, p. 126377, 2021/09/15/ 2021, doi: https://doi.org/10.1016/j.jhazmat.2021.126377.
158. D. T. Li, H. Yu, and Y. Huang, "Facile H(2)PdCl(4)-induced photoreforming of insoluble PET waste for C1-C3 compound production," *Front Chem,* vol. 11, p. 1265556, 2023, doi: 10.3389/fchem.2023.1265556.
159. K. Bule Možar *et al.*, "Evaluation of Fenton, Photo-Fenton and Fenton-like Processes in Degradation of PE, PP, and PVC Microplastics," *Water,* vol. 16, no. 5, p. 673, 2024. [Online]. Available: https://www.mdpi.com/2073-4441/16/5/673.
160. M. Surana, D. S. Pattanayak, V. Yadav, V. K. Singh, and D. Pal, "An insight decipher on photocatalytic degradation of microplastics: Mechanism, limitations, and future outlook," *Environmental Research,* vol. 247, p. 118268, 2024/04/15/ 2024, doi: https://doi.org/10.1016/j.envres.2024.118268.
161. Y. Pan *et al.*, "Removing microplastics from aquatic environments: A critical review," (in eng), *Environ Sci Ecotechnol,* vol. 13, p. 100222, Jan 2023, doi: 10.1016/j.ese.2022.100222.
162. A. Xie, M. Jin, J. Zhu, Q. Zhou, L. Fu, and W. Wu, "Photocatalytic Technologies for Transformation and Degradation of Microplastics in the Environment: Current Achievements and Future Prospects," *Catalysts,* vol. 13, no. 5, p. 846, 2023. [Online]. Available: https://www.mdpi.com/2073-4344/13/5/846.

 doi:10.20944/preprints202504.1506.v1

163. P. Chattopadhyay, M. C. Ariza-Tarazona, E. I. Cedillo-Gonzalez, C. Siligardi, and J. Simmchen, "Combining photocatalytic collection and degradation of microplastics using self-asymmetric Pac-Man TiO(2)," *Nanoscale,* vol. 15, no. 36, pp. 14774-14781, Sep 21 2023, doi: 10.1039/d3nr01512b.
164. B. E. Llorente-García, J. M. Hernández-López, A. A. Zaldívar-Cadena, C. Siligardi, and E. I. Cedillo-González, "First Insights into Photocatalytic Degradation of HDPE and LDPE Microplastics by a Mesoporous N–TiO2 Coating: Effect of Size and Shape of Microplastics," *Coatings,* vol. 10, no. 7, p. 658, 2020. [Online]. Available: https://www.mdpi.com/2079-6412/10/7/658.
165. B. Ramasubramanian, J. Tan, V. Chellappan, and S. Ramakrishna, "Recent Advances in Extended Producer Responsibility Initiatives for Plastic Waste Management in Germany and UK," *Materials Circular Economy,* vol. 5, no. 1, 2023, doi: 10.1007/s42824-023-00076-8.
166. U. S. D. o. Energy. "Hydrogen Laws and Incentives in Federal." (accessed.
167. T. Uekert, M. A. Bajada, T. Schubert, C. M. Pichler, and E. Reisner, "Scalable Photocatalyst Panels for Photoreforming of Plastic, Biomass and Mixed Waste in Flow," (in eng), *ChemSusChem,* vol. 14, no. 19, pp. 4190-4197, Oct 5 2021, doi: 10.1002/cssc.202002580.
168. J. Ran, A. Talebian-Kiakalaieh, S. Zhang, E. M. Hashem, M. Guo, and S. Z. Qiao, "Recent advancement on photocatalytic plastic upcycling," *Chem Sci,* vol. 15, no. 5, pp. 1611-1637, Jan 31 2024, doi: 10.1039/d3sc05555h.
169. T. K. A. Nguyen *et al.*, "Understanding Structure-Activity Relationship in Pt-loaded g-C(3) N(4) for Efficient Solar- Photoreforming of Polyethylene Terephthalate Plastic and Hydrogen Production," (in eng), *Small Methods,* vol. 8, no. 2, p. e2300427, Feb 2024, doi: 10.1002/smtd.202300427.
170. R. Wei *et al.*, "Photocatalytic Upgrading of Plastic Waste into High-Value-Added Chemicals and Fuels: Advances and Perspectives," *ACS Sustainable Chemistry & Engineering,* vol. 13, no. 7, pp. 2615-2632, 2025/02/24 2025, doi: 10.1021/acssuschemeng.4c09610.
171. J. M. Carceller, K. S. Arias, M. J. Climent, S. Iborra, and A. Corma, "One-pot chemo- and photo-enzymatic linear cascade processes," *Chem Soc Rev,* vol. 53, no. 15, pp. 7875-7938, Jul 29 2024, doi: 10.1039/d3cs00595j.
172. M. Daboczi, "Virtually free clean hydrogen generation by photoelectrochemical devices?," *Matter,* vol. 6, no. 8, pp. 2594-2596, 2023, doi: 10.1016/j.matt.2023.06.036.
173. Q. Li, L.-G. Wang, and J.-B. Wu, "Recent advances in dual-atom catalysts for energy catalysis," *Rare Metals,* vol. 44, no. 2, pp. 841-867, 2025/02/01 2025, doi: 10.1007/s12598-024-02911-6.
174. X. Wang *et al.*, "Developing a class of dual atom materials for multifunctional catalytic reactions," *Nature Communications,* vol. 14, no. 1, p. 7210, 2023/11/08 2023, doi: 10.1038/s41467-023-42756-8.
175. E. Wang, M. Guo, J. Zhou, and Z. Sun, "Reasonable Design of MXene-Supported Dual-Atom Catalysts with High Catalytic Activity for Hydrogen Evolution and Oxygen Evolution Reaction: A First-Principles Investigation," *Materials,* vol. 16, no. 4, p. 1457, 2023. [Online]. Available: https://www.mdpi.com/1996-1944/16/4/1457.
176. E. M. N. T. Edirisooriya, P. S. Senanayake, P. Xu, and H. Wang, "Recyclability and regeneration of Au/TiO2 nanocomposite and Pt/TiO2 atom-nano composite catalysts in photo-reforming plastics for hydrogen production," *Journal of Environmental Chemical Engineering,* vol. 13, no. 3, p. 116467, 2025/06/01/ 2025, doi: https://doi.org/10.1016/j.jece.2025.116467.
177. M. M. Khan, A. Rahman, and S. N. Matussin, "Recent Progress of Metal-Organic Frameworks and Metal-Organic Frameworks-Based Heterostructures as Photocatalysts," (in eng), *Nanomaterials (Basel),* vol. 12, no. 16, Aug 17 2022, doi: 10.3390/nano12162820.
178. H. Yang, J. Xu, H. Cao, J. Wu, and D. Zhao, "Recovery of homogeneous photocatalysts by covalent organic framework membranes," *Nature Communications,* vol. 14, no. 1, p. 2726, 2023/05/11 2023, doi: 10.1038/s41467-023-38424-6.
179. S. R. Kavanagh, "Accurately Modelling Point Defects in Semiconductors: The Case of CdTe," Doctor of Computational Materials Science, Department of Chemistry (UCL) & Department of Materials (ICL), University College London & Imperial College London, 2024.

 doi:10.20944/preprints202504.1506.v1

180. F. Frieden and J. Leker, "Future costs of hydrogen: a quantitative review," *Sustainable Energy & Fuels*, vol. 8, no. 9, pp. 1806-1822, 2024, doi: 10.1039/d4se00137k.
181. T. Ahasan, E. M. N. T. Edirisooriya, P. S. Senanayake, P. Xu, and H. Wang, "Advanced TiO2-Based Photocatalytic Systems for Water Splitting: Comprehensive Review from Fundamentals to Manufacturing," *Molecules*, vol. 30, no. 5, 2025, doi: 10.3390/molecules30051127.